

DEVELOPMENT OF THE HYDROCOPTER
AUTONOMOUS UNDERWATER VEHICLE

RAJENDRA JANI

DEVELOPMENT OF THE HYDROCOPTER
AUTONOMOUS UNDERWATER VEHICLE

by

RAJENDRA JANI, P.Eng

A thesis submitted to the School of Graduate
Studies in partial fulfillment of the requirements for
The Degree of Masters of Engineering

Faculty of Engineering and Applied Science
Memorial University of Newfoundland
March 2006

St. John's

Newfoundland

Canada



Library and
Archives Canada

Bibliothèque et
Archives Canada

Published Heritage
Branch

Direction du
Patrimoine de l'édition

395 Wellington Street
Ottawa ON K1A 0N4
Canada

395, rue Wellington
Ottawa ON K1A 0N4
Canada

Your file *Votre référence*
ISBN: 978-0-494-30526-3
Our file *Notre référence*
ISBN: 978-0-494-30526-3

NOTICE:

The author has granted a non-exclusive license allowing Library and Archives Canada to reproduce, publish, archive, preserve, conserve, communicate to the public by telecommunication or on the Internet, loan, distribute and sell theses worldwide, for commercial or non-commercial purposes, in microform, paper, electronic and/or any other formats.

The author retains copyright ownership and moral rights in this thesis. Neither the thesis nor substantial extracts from it may be printed or otherwise reproduced without the author's permission.

AVIS:

L'auteur a accordé une licence non exclusive permettant à la Bibliothèque et Archives Canada de reproduire, publier, archiver, sauvegarder, conserver, transmettre au public par télécommunication ou par l'Internet, prêter, distribuer et vendre des thèses partout dans le monde, à des fins commerciales ou autres, sur support microforme, papier, électronique et/ou autres formats.

L'auteur conserve la propriété du droit d'auteur et des droits moraux qui protègent cette thèse. Ni la thèse ni des extraits substantiels de celle-ci ne doivent être imprimés ou autrement reproduits sans son autorisation.

In compliance with the Canadian Privacy Act some supporting forms may have been removed from this thesis.

Conformément à la loi canadienne sur la protection de la vie privée, quelques formulaires secondaires ont été enlevés de cette thèse.

While these forms may be included in the document page count, their removal does not represent any loss of content from the thesis.

Bien que ces formulaires aient inclus dans la pagination, il n'y aura aucun contenu manquant.


Canada

To Daxa and my family

SUMMARY

This thesis deals with the development of a small high-speed autonomous underwater vehicle or AUV known as the Hydrocopter that can mimic the motion of a helicopter. A model was designed and constructed. It was tested in the Deep Water Tank at Memorial University. A SIMULINK simulation of the AUV was developed to study its underwater motions. The simulation and test responses show that the AUV can move at high speed along any 3D trajectory.

ACKNOWLEDGMENTS

The author wishes to thank Dr. Michael Hinchey for his unyielding support throughout the project from the concept stage to final testing. I am particularly indebted to him for his guidance in control selection strategy and simulation not to mention allowing access to laboratory facilities during build and subsequent tests. I would also like to extend my thanks to the Technical Services Department at MUN, MTC at MUN (Mr. Healey in particular), MTC at the College of the North Atlantic (Mr. Stephen Hicks, Mr. Neil Piercy, Mr. M. Ingermann and Miss L. Hibbs) and the Fluids and Thermodynamics laboratory staff at MUN (Mr. Jim Gosse). The audiovisual departments of MUN, Marine Institute (Mr. K Butler) and College of the North Atlantic (Mr. H. Baker) provided valuable assistance in editing and preparing video and CD's of testing.

TABLE OF CONTENTS

SUMMARY		iii
ACKNOWLEDGMENTS		iv
LIST OF FIGURES		vii
CHAPTER 1	INTRODUCTION	1
CHAPTER 2	UNDERWATER VEHICLES REVIEW	3
	2.1 Preamble	3
	2.2 Remotely Operated Vehicles Or Rovs	3
	2.3 Autonomous Underwater Vehicles Or Auvs	4
	2.4 Auvs At Memorial University	6
CHAPTER 3	DESIGN OF UNDERWATER VEHICLES	11
	3.1 Preamble	11
	3.2 Control Of Underwater Vehicles	12
	3.2.1 Overview Of Control Theories	12
	3.2.2 Error Driven Control	13
	3.2.3 Controllers For Underwater Vehicles	21
	3.3 Fins And Propellors	21
	3.3.1 Steady Foil Theory	21
	3.3.2 Unsteady Foil Theory	22
	3.3.3 Finite Span Phenomena	23
	3.4 Underwater Vehicle Motors	24
	3.5 Underwater Vehicle Structures	26
	3.6 Energy System	29
	3.7 Buoyancy	30

CHAPTER 4	SIMULINK DYNAMICS SIMULATION	31
CHAPTER 5	HYDROCOPTER MODEL	41
	5.1 Design Criteria	41
	5.2 Hydrocopter Model Components	41
	5.2.1 Model Body	42
	5.2.2 Energy Storage System	42
	5.2.3 Propulsion System	43
	5.2.4 Sensors	43
	5.2.5 Control System	44
	5.2.6 Control Code	44
CHAPTER 6	RESULTS OF SIMULATION & TESTS	52
CHAPTER 7	CONCLUSIONS AND FUTURE WORK	60
REFERENCES		61
APPENDIX A	ESTIMATION OF HYDROCOPTER PARAMETERS	64
APPENDIX B	SPECIFICATION SHEETS FOR VARIOUS COMPONENTS	69

LIST OF FIGURES

1.1	Assembled Hydrocopter Model	2
2.1	Typical ROV	4
2.2	Typical AUV	5
2.3	APEX	6
2.4	Global Underwater Surveyor (GUS)	7
2.5	AUV Under Development at MUN	8
2.6	Submersible Escape Capsule	9
2.7	C-Scout	10
3.1	Block Diagram of Typical Feedback Control System	15
3.2	12 Volt DC Motor	24
3.3	Example of Laminar Flow Hull	27
3.4	Example of Torpedo Body Hull	28
4.1	Overall Block Diagram	34
4.2	Control Subblock	35
4.3	Surge Subblock	36
4.4	Pitch Subblock	37
4.5	Yaw Subblock	38
4.6	Heave Subblock	39
4.7	XY Subblock	40

5.1	Omega Pressure Sensor	45
5.2	IC Sensors Accelerometer	45
5.3	Control Circuit	47
5.4	Control Chart	51
6.1	3D Plot of Hydrocopter Simulation	53
6.2	Test Tank	54
6.3	Computer Animation of Vertical Motion	56
6.4	Vertical Motion Test in Tank	57
6.5	Computer Animation of Horizontal Motion of the Hydrocopter	58
6.6	Robot in Horizontal Motion during Test	59

CHAPTER 1

INTRODUCTION

The two major types of underwater vehicles are: remotely operated vehicles (ROVs) and autonomous underwater vehicles (AUVs). None currently available can move at high speed along a complex 3D trajectory. This thesis deals with the development of an AUV known as the Hydrocopter. The goal was to develop an AUV that could fly at high speed along any 3D trajectory. A model was designed and constructed. A photograph of this model is given in Figure 1.1 It uses two variable speed propellers at the bow to control surge and yaw motions and a fin at the stern to control pitch and heave motions.

The thesis is divided into seven Chapters. Chapter 1 gives some background and discusses the goal of the project. Chapter 2 gives a review of the state of the art of underwater vehicle technology. Chapter 3 gives the background needed to design the Hydrocopter. Chapter 4 gives the details of a SIMULINK simulation. Chapter 5 gives the details of the model Hydrocopter design and construction. Chapter 6 gives results of simulation and

tank tests. Chapter 7 gives conclusions and recommendations for future work.

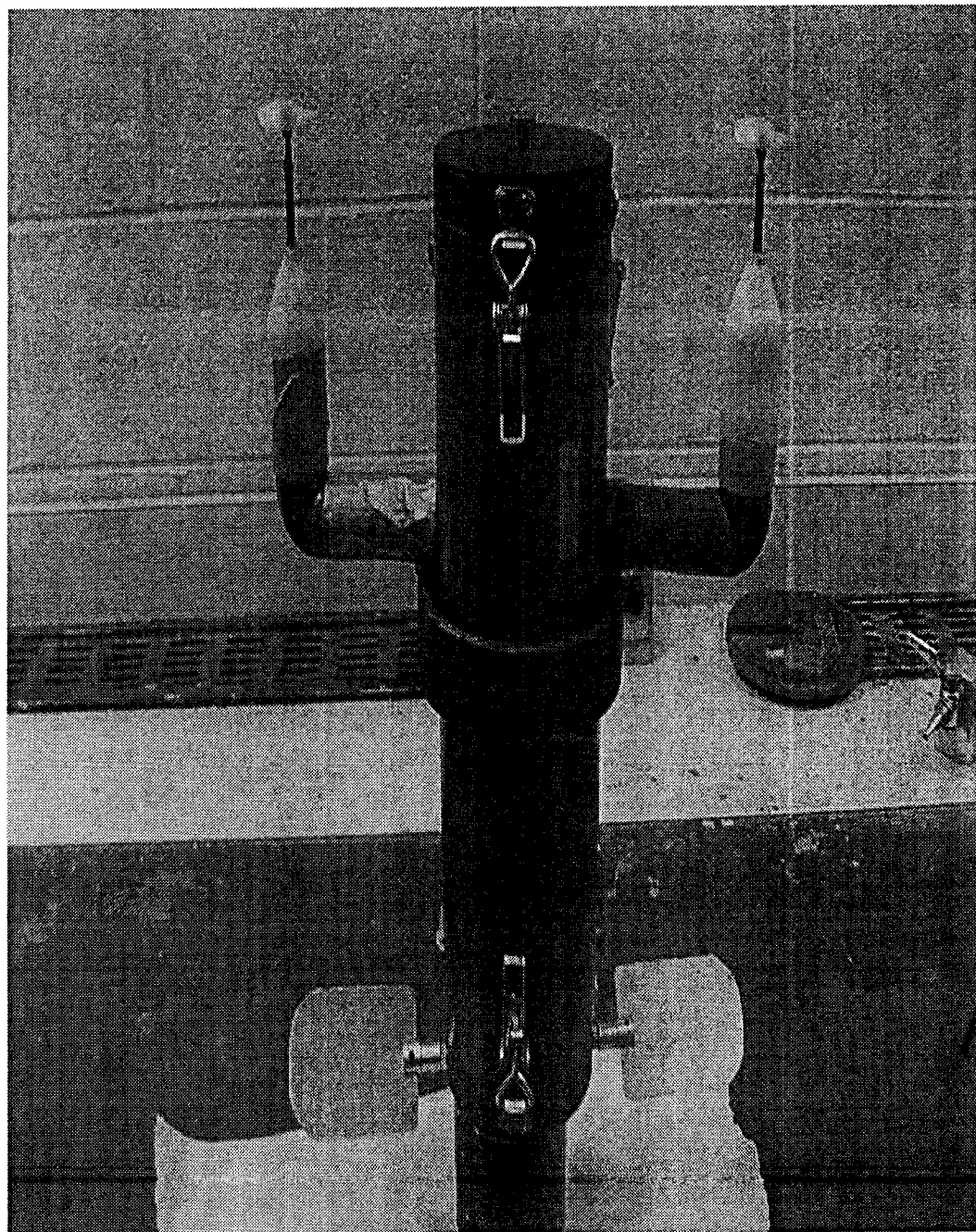


Figure 1.1 Assembled Hydrocopter Model

CHAPTER 2

UNDERWATER VEHICLES REVIEW

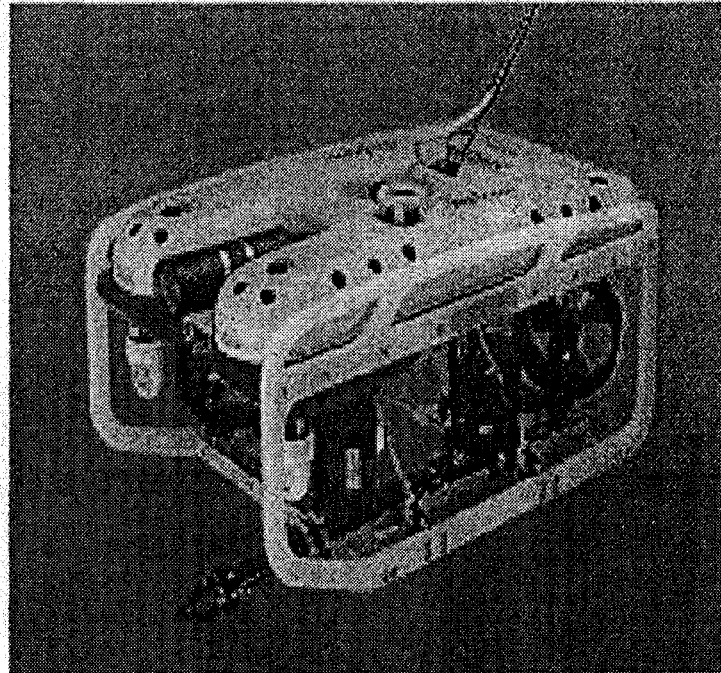
2.1 Preamble

This chapter gives a review of underwater vehicles currently in use around the world. The focus is on systems and not on research. There are two types of underwater vehicles: Remotely Operated Vehicles or ROVs and Autonomous Underwater Vehicles or AUVs.

2.2 Remotely Operated Vehicles or ROVs

ROVs are generally connected to a host ship by an umbilical cable. This cable supplies power to drives and sensors on the ROV. A human operator on the host ship can receive and send signals from sensors and drives. Sensors include a compass for heading information, a solid state gyro for auto heading control and a depth sensor for information in feet or meters, while drives include velocity feedback for precise and rapid thrust control. ROVs are usually used for inspection of offshore structures and for installation of devices. They generally have a box frame construction, which is not very hydrodynamically clean. However the box frame is not a problem because ROVs

generally do not have to travel long distances or at high speed and basically have unlimited supply of power. A typical ROV in use today offshore is shown in Figure 2.1.



Seaeye Falcon

Figure 2.1 Typical ROV

2.3 Autonomous Underwater Vehicles or AUVs

AUVs use an onboard computer for control. They are generally not connected to a host ship and do not have an unlimited supply of power. Most AUVs have a torpedo like shape. AUV technology is not as well developed as ROV technology. AUVs are being used mainly for inspection and

survey missions. A typical AUV in use today offshore is shown in Figure 2.2.



Figure 2.2 Typical AUV

Some AUVs drift with local current but can move vertically through the water column. They are used by scientists who study the oceans. Several dozen drifters known as ALACE (Autonomous Lagrangian Circulation Explorer) are presently deployed in the Labrador current. They use a piston to control displaced volume and thus buoyancy, they can also stay submerged for several months. Periodically they come up to the ocean surface and upload data to

satellites. A photograph of a drifter known as APEX is given below.

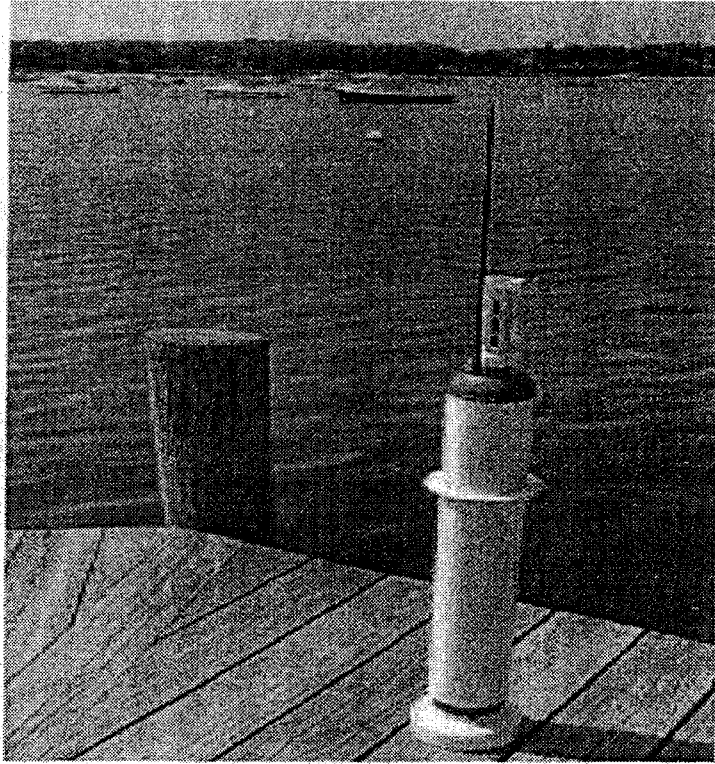


Figure 2.3 APEX

2.4 AUVs at Memorial University

MUN is developing a drifter known as GUS (Global Underwater Surveyor), which uses an air/water ballast tank for depth control. A photo of GUS is shown below (figure 2.4). An earlier version of GUS was called NO MAD (meaning NOT MAD).

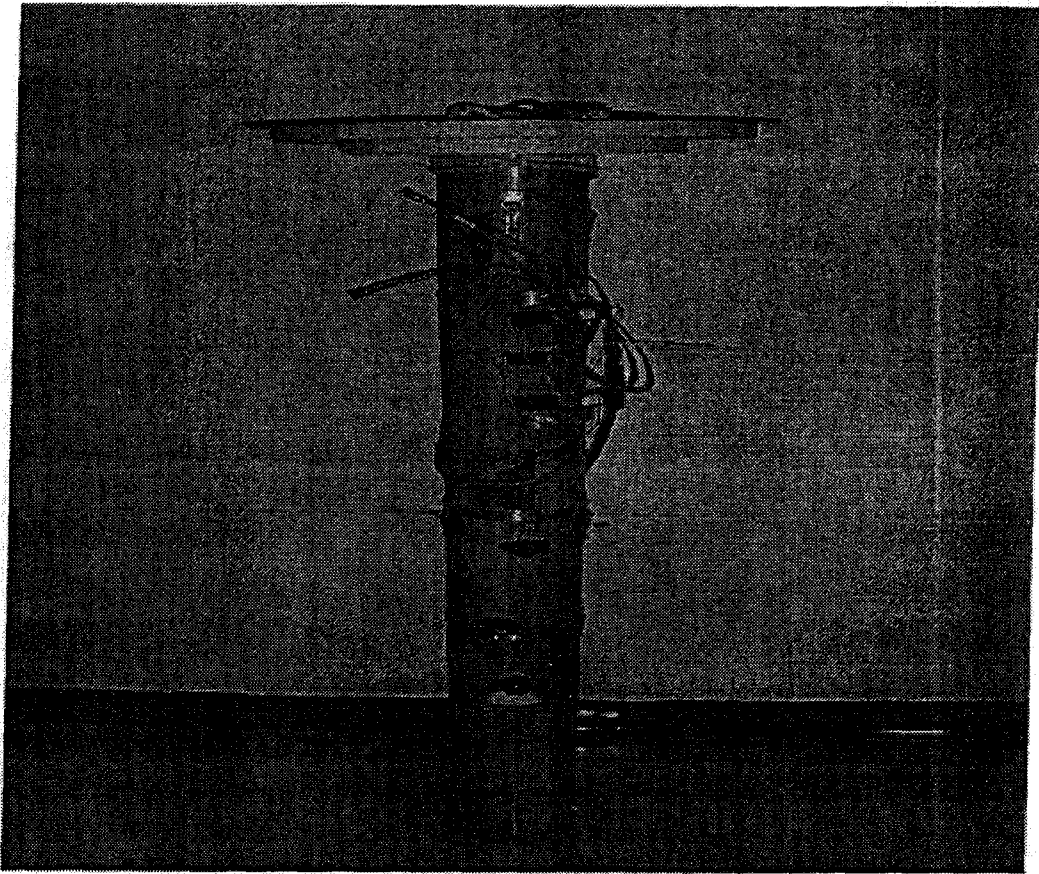


Figure 2.4 Global Underwater Surveyor (GUS)

AUVs are generally very expensive, however MUN is developing a series of much less expensive vehicles. Each vehicle is very modular and can be easily assembled or disassembled. Each makes use of the same controller and propulsion units. A vehicle that was recently tested is shown in a photo below (Figure 2.5). It uses two trolling motors at the front to control surge and yaw and another motor at the rear to control pitch. The front motors hang

like the engines from a jet aircraft. Cost of this AUV is less than Five Thousand Canadian Dollars.

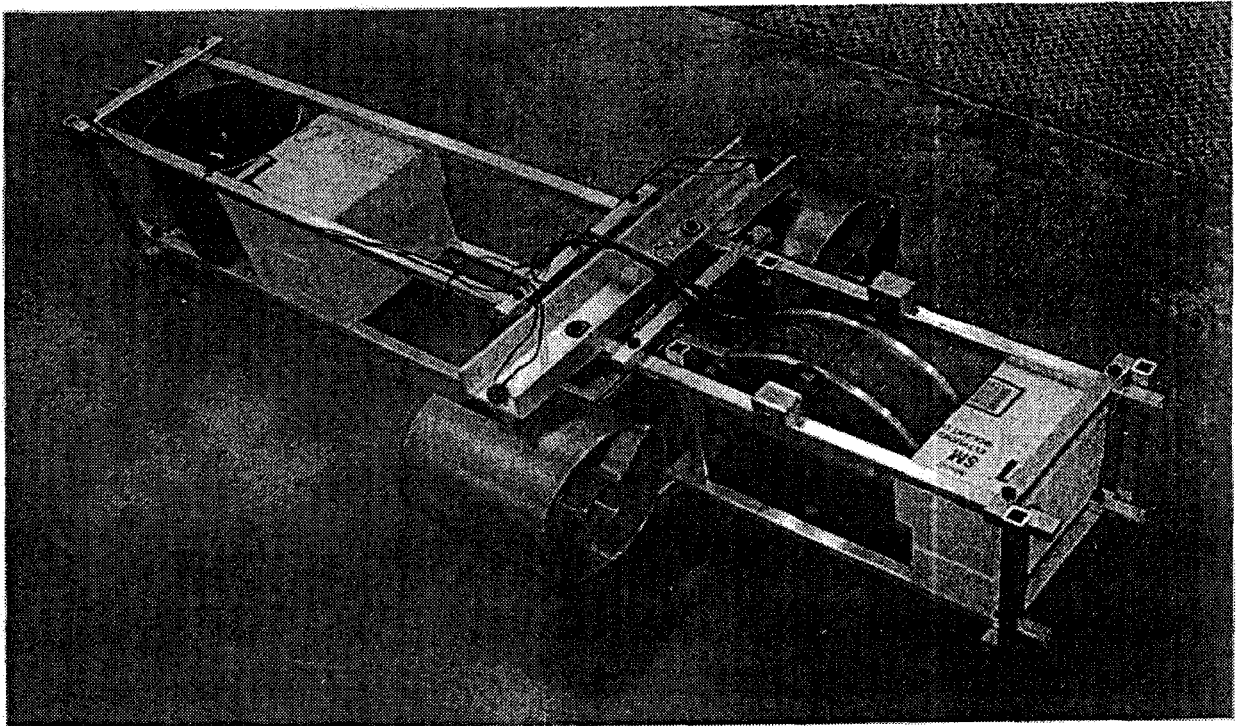


Figure 2.5 AUV Under Development at MUN

Most evacuation systems currently in use on offshore structures are inadequate. Typically, they are damaged by contact with the structure during launch. MUN is developing a submersible escape capsule that avoids the contact problem. Its underwater motion would be controlled automatically. A model capsule is shown in the photo below (Figure 2.6).



Figure 2.6 Submersible Escape Capsule

MUN is also developing a torpedo shaped AUV known as C-SCOUT for survey type missions related to oil and gas production. A photo of this vehicle is shown in the photo below (Figure 2.7). MUN is also developing a glider AUV which uses fins and a buoyancy engine to follow a 3D trajectory.

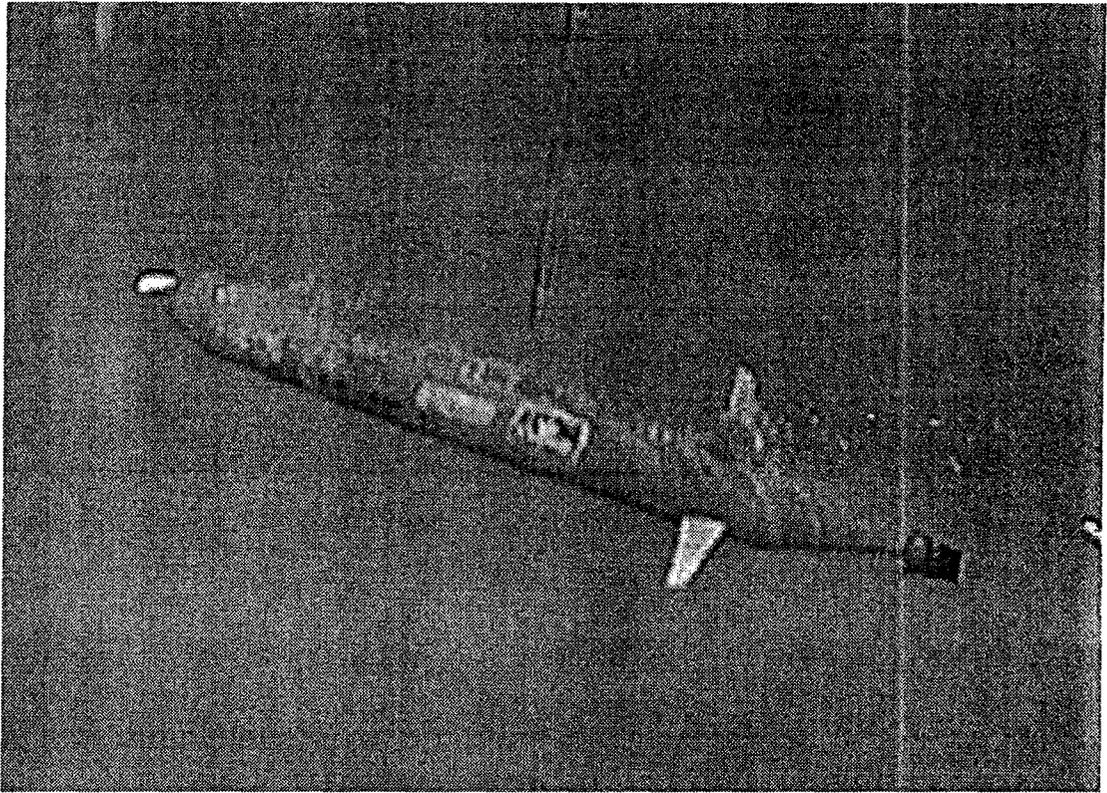


Figure 2.7 C-Scout

CHAPTER 3

DESIGN OF UNDERWATER VEHICLES

3.1 Preamble

This chapter describes the factors that must be considered to design an underwater vehicle. To conserve energy, an underwater vehicle must be neutrally buoyant, and at zero pitch or trim angle, its center of gravity (CG) must be directly below its center of buoyancy. Simple hydrostatics can be used to design a vehicle which has these characteristics [Allmendinger 1990]. To move an underwater vehicle through the water at a command steady speed, its thrusters must have sufficient power. Simple drag calculations can be used to size the thrusters, because when a vehicle is moving at a command steady speed, thrust equals drag. To maneuver an underwater vehicle in a desired way, thrusters and control surfaces must be positioned properly.

The equations governing the motion of a general underwater vehicle are a complex set of six coupled ordinary differential equations. They contain three translation degrees of freedom (heave, surge, sway) and three rotational degrees of freedom (roll, pitch, yaw).

The equations contain many parameters, which often can only be obtained from sophisticated experiments. Usually, there is inertia coupling of degrees of freedom. There can also be coupling due to hydrodynamic loads. These loads include: pressure and inertia loads, wake, wall, and wave drag loads. The Hydrocopter design is such that there is very little coupling. This greatly simplifies its dynamics and ensures that it can be designed to be statically and dynamically stable.

3.2 Control of Underwater Vehicles

The Hydrocopter is basically an autonomous underwater vehicle. One could consider it to be a subsea robot. Control of such robots is reviewed below [Hinchey 2004].

3.2.1 Overview of Control Theories

There are many different types of control strategies (Franklin, Powell, Emami-Naeini, 2006). Examples include: classical feedback control; state space or modern control; digital or discrete control; optimal control; stochastic control; adaptive control; robust control; computed load control; sliding mode control; infinite degree of freedom control; supervisory control. We will not review all of these here. Supervisory control tries to mimic a human

operator. It usually operates at a higher level than error driven control. It often picks things like gains and targets for such control.

A popular control strategy for exploration robots is the layered strategy known as subsumption. This was developed by Brooks and his colleagues at MIT. Each layer in subsumption is basically a behaviour. For the most part, layers operate independently of each other. However, top layers have higher priority and take over or subsume control from lower layers when conditions warrant. For example, a lower layer might try to keep an exploration subsea robot a certain distance above the bottom. However, when the robot approaches an underwater cliff, a higher layer would take over to get the robot over the cliff and then pass control back to the appropriate lower layer. So, the surroundings determine the nature of control. The MIT group claims that subsumption gives robots insect like intelligence: making them react to surroundings much like insects.

3.2.2 Error Driven Control

The Hydrocopter uses classical feedback control. Figure 3.1 shows a typical feedback control system. What has to be controlled is generally referred to as the plant.

What the plant is doing is known as its response. What it should be doing is known as the command. The plant receives a control signal from a drive and a disturbance signal from the surroundings. The goal is to pick a controller that can make the response follow closely command signals but reject disturbances. The controller acts on an error signal: this is command minus some measure of the response, known as error driven control. Two types of error driven control are Proportional Integral Derivative (PID) and Switching. Proportional generates a signal which is proportional to error. Integral generates a signal which is proportional to the integral of the error. Derivative generates a signal which is proportional to the rate of change of error. Switching generally gives out signals with constant levels.

Each degree of freedom of the Hydrocopter subsea robot is governed by an equation of the form :

$$X \frac{d^2R}{dt^2} + Y \frac{dR}{dt} + Z |dR/dt| + K R = B + D$$

where R is the degree of freedom , X is its inertia, Y accounts for wake drag, Z accounts for wall drag, K accounts for spring like loads, B is a drive load and D is a disturbance load.

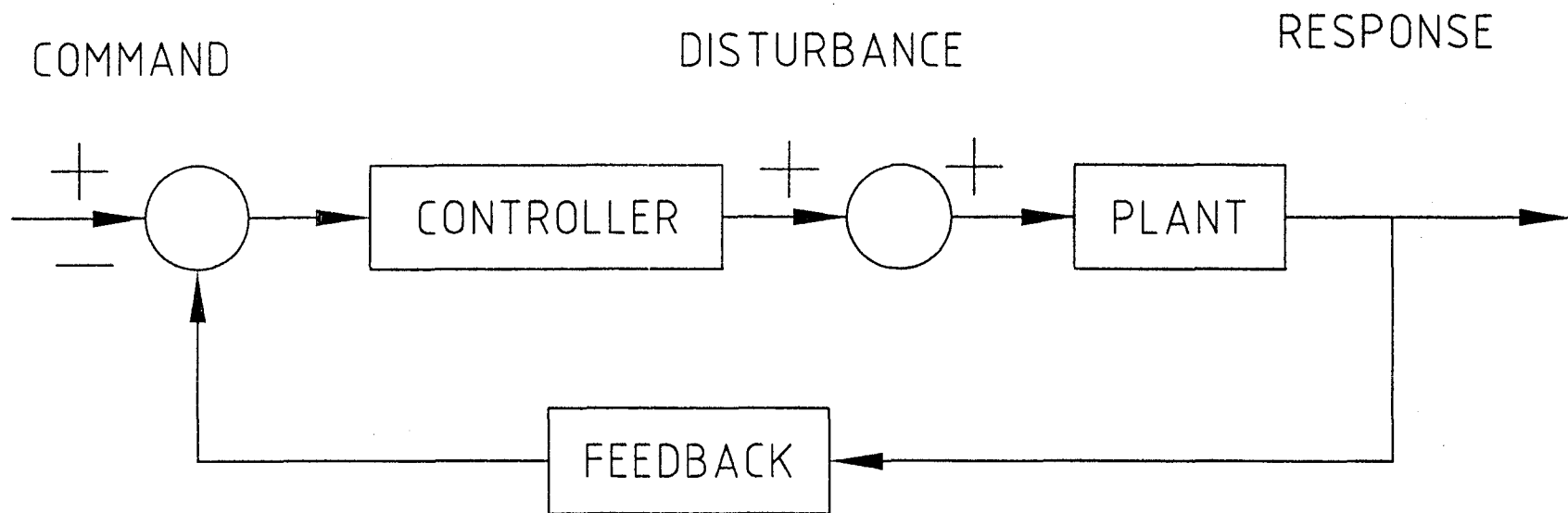


Figure 3.1 Block Diagram of a Typical Feedback Control System

A simple model for a drive is:

$$J \frac{dB}{dt} + I B = Q$$

where Q is a drive signal. The Hydrocopter subsea robot uses motor driven propellers to generate B : I accounts for the size and shape of the blades while J accounts for things like rotor inertia. One could determine J and I experimentally. Drive dynamics would cause the drive load to lag the drive signal. The amount of lag depends on how large J is relative to I . Consider the case where proportional control is acting alone and the error is initially positive. For a slowly reacting propulsion system, positive error would cause a positive load to gradually build up. As it builds up, this load would move the robot towards the command depth. However, when the robot gets to the command depth, the control load would still be positive, and this would cause overshoot. In some cases, these overshoots would settle down. In other cases, they would not settle down but would limit because of wake drag.

Small subsea robots would be controlled by small onboard computers. Control signals would be generated within a computer control loop. The loop period must be much smaller than the basic period of robot motion: otherwise severe overshoots could develop. If the subsea robot was controlled remotely by a computer onboard a ship, the time taken for the

depth signal to travel from the robot to the ship and the time taken for the drive signal to travel back from the ship to the robot could cause overshoots, because the robot would be responding to past error not present error.

To illustrate the various strategies, we will focus only on the heave degree of freedom. Imagine that a subsea robot is at the water surface and it is suddenly commanded to go to some constant command depth C . Assume that there is a disturbance with a constant level D acting downward.

The PID strategy lets the drive signal Q be:

$$Q = K_P E + K_I \int E d\tau + K_D dE/dt$$

where $E = C - R$ is the depth error: R is the actual depth and C is the command depth. The controller gains are: K_P K_I K_D .

Proportional by itself would cause the propellers to spin in such a way that the robot would move towards the command depth. The amount of spin would be proportional to depth error. When the vehicle reaches the command depth, the proportional control signal would be zero. If the robot was held at the command depth, its propellers would stop spinning. The disturbance would cause the robot to stop below the command depth. This offset would be such that the propellers generate just enough upward force to balance the downward disturbance. The offset would be DI/K_P . When D is

known, something called feedforward compensation can be used to get rid of the offset. Basically, we measure D and subtract ID from Q in the drive equation. When motions settle down, the drive gives out an extra force minus D which cancels D , but we must know D . Another way to get rid of the offset is to give the robot a false command C^* . If the false command C^* was set at $C - DI/K_p$, the robot would end up at C . It would hang below C^* by DI/K_p and thus end up at C . If the gain K_p was very large, offsets such as DI/K_p would probably be tolerable. However, large gain would generate very large Q when the depth is well away from the command depth. Very large Q could burn out drives. To avoid this, a limit is usually put on the magnitude of Q . In this case, the control is referred to as proportional with saturation. If the disturbance was greater than the saturation limits, then control would be impossible.

Integral by itself would cause the propellers to spin in such a way that the robot would move towards the command depth. The amount of spin would be proportional to the integral of depth error. As the robot moves toward the command depth, the propellers would spin faster and faster. Obviously, this would cause the robot to overshoot the command depth. Because of these overshoots, integral cannot be used alone. The good thing about integral is it gives zero offsets. If the robot was held with positive depth error, the

integral control signal would get bigger and bigger. This is known as integral windup. If it was released after a long time, it would take a very large integrated negative error to cancel out the windup due to integrated positive error. A simple way to avoid integral windup is to activate integral only within a band surrounding the command depth. All we need is for the band to be wide enough for proportional to get the robot within the band so that integral can home it into the command depth.

Derivative by itself cannot be used alone. Assume that the command C is a constant, and let the robot be stopped far away from the command depth. In this case, dE/dt would be zero. So, the controller would not generate a force to move the robot to the command depth. Derivative control mimics drag load and helps motions settle down. It generates a drive load which opposes motion. Something called, "rate feedback" could also be used to help make motions settle down. The controller would act on depth error, E minus a constant times the depth rate dR/dt . Substitution into the governing equations shows that rate feedback mimics drag. Note that derivative control could be used to make the robot move at a constant speed. For this, dC/dt is made a constant. Drag and the dR/dt part of dE/dt would tend to limit speed.

With all three components of PID acting together, as soon as the robot passes through the command depth, proportional would tend to counteract integral. Also, proportional would get the robot closer to the command depth faster, so it would limit integral windup. Derivative would help counteract overshoots. The robot would home in quickly on the command depth with minimal overshoots. So, we achieve good characteristics of all three controllers.

Ziegler and Nichols (Franklin,2006), through a series of experiments on simple systems, developed criteria for picking gains in a PID controller that would give good tracking performance. For a system that can be made unstable with proportional acting alone, the recommended procedure for getting a reasonable set of gains is as follows. With proportional acting alone, increase its gain until the system becomes borderline stable. Let the borderline stable gain be K_P and its period be T_P . According to Ziegler Nichols, reasonable gains are:

$$K_P = 0.6K_P \quad K_I = K_P/T_I \quad K_D = K_P*T_D$$

where

$$T_I = T_P/2.0 \quad T_D = T_P/8.0$$

are integral and derivative time constants. Ziegler Nichols gains in the present work was not used.

3.2.3 Controllers for Underwater Vehicles

The Hydrocopter uses a small onboard controller to control its motion. There are many controllers available that could have been used for this task. For example, the RUGGED GIANT Controller and the RABBIT Controller developed by Z WORLD ENGINEERING could have been used but have capabilities way beyond what was needed for the present work. Instead, special circuits based on the Peripheral Interface Controller or PIC were developed for the Hydrocopter. This is described in greater detail in Chapter 5.

3.3 Fins and Propellers

The Hydrocopter uses bow propellers for surge and yaw control. It uses a stern fin for pitch and heave control. Basic theory for such devices is reviewed below.

3.3.1 Steady Foil Theory

Sections of fins or propellers are known as foils. One can break a fin or propellor into strips and use foil theory to analyze each strip. Superposition can then be used to estimate the total loads. There are two lift theories for steady foils. Both are based on potential flow concepts. One theory superimposes a stream with a doublet to get a circular dividing streamline. A vortex is then

superimposed onto this flow. The flow is then mapped to get the flow around a foil. The foils generated are basically sections of fins. The strength of the vortex is adjusted to make the trailing edge a stagnation point. This makes the flow leave the edge smoothly like it is observed to do on real foils well away from stall. The vortex speeds the flow up on the top and slows it down on the bottom. This creates suction or negative pressure on top and positive pressure on the bottom. Without the vortex, lift is zero! The second theory for steady foils superimposes a stream with an infinite number of infinitesimal strength vortices distributed along the mean camber line of the foil. Its foils are basically sections of propellers. An infinite number of vortices can generate complex foil shapes like those on propellers. Details of foil theory may be found in *Applied Hydro and Aeromechanics* by Prandtl and Tietjens, 1934 and *Fluid Mechanics with Engineering Applications* by Finnemore and Franzini, 2002.

3.3.2 Unsteady Foil Theory

For a foil undergoing heave or pitch motions, the circulation around the foil must change continuously to keep the flow realistic at the trailing edge. Every time

the circulation changes, an equal and opposite amount of circulation must shed behind the foil, and this is carried downstream by the passing stream. For arbitrary foil motions, it is customary to lump that shed over a small segment of time into a point vortex. These vortices modify the flow over the foil and thus its lift. This is done by creating upwashes or downwashes depending on how the vortices are spinning. The details of this are beyond this thesis.

3.3.3 Finite Span Phenomena

Vortices can only end at a wall or form loops. For steady flow over a fin or propellor, horseshoe shaped vortices are shed along the span because circulation varies along the span. These vortices are strongest at the tips of the fin or propellor. They are carried downstream by the passing stream. If there was no viscosity, the vortices would complete a loop back where the fin or propeller first began to move. However, they are dissipated by friction before they can do this. The horseshoe vortices create an upwash or downwash depending on which way they are rotating and this changes the angle of attack of the fin or propeller along its span. This in turn changes the lift and

drag of the fin or propellor. The strength of the horseshoe vortices is determined by the circulation on the fin or propeller. The details of this are beyond this thesis.

3.4 Underwater Vehicle Motors

The propellers on the Hydrocopter are driven by two 12V, 1.5 A current max, with 11500 rpm (with load) DC motors. Torque is generated in these motors by the interaction of magnetic fields generated by permanent magnets and energized coils of wire. Figure 3.2 shows the type of motor used on the Hydrocopter.

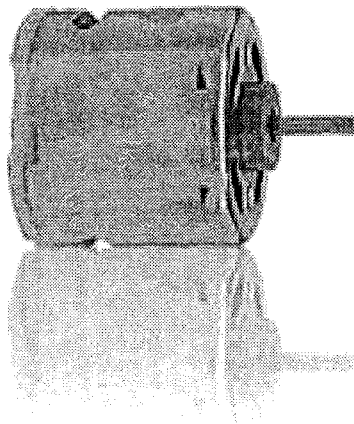


Figure 3.2 12V DC Motor

There are two methods of modulating DC power to control motor speed. One method is to use resistors to burn off a portion of the supplied power or use operational amplifiers to regulate DC, however this method is wasteful. The other method is to use "switched" power supply, which is called Pulse Width Modulation (PWM). In PWM, the load is rapidly connected and disconnected from the supply; there is never any need to burn off part of the supplied power. If full power is supplied to the motor only half the time, the motor runs at the speed at which it would run if half power was applied. The width of the "on" pulses can be varied, or "modulated," so that average power to the motor is anywhere from fully off to fully on. The Hydrocopter uses PWM to regulate motor speed.

DC motors are widely used in small underwater vehicles because they are small, cheap and easy to work with. They have unloaded speeds in the range of 3,000 to 24,000 rpm, 9Vdc - 18V dc, 380 - 430 mA unloaded current (1.1 - 2.4 A loaded). They have a range of 150g.cm min - 290g.cm min. torque. Commercial AUV's such as the AUTOSUB use brushless DC motors driving five bladed propellers with no reduction gearing and seawater lubricated bearings. Commercial ROV's such as the Seaeye Falcon have developed the innovative

magnetically coupled brushless DC thruster which is capable of resisting higher torque loads than the ordinary brushless thrusters. Each thruster is capable of achieving 13 kgf thrust at 320 W. These thrusters are interfaced to a fast PID control system along with a solid - state rate gyro for azimuth stability, a feature that automatically prevents overshoot on a change of heading.

3.5 Underwater Vehicle Structures

Many underwater vehicle structures are simple and can be designed by simple structural theories. For example, pinned box section tubes are easy to design. Other structures like cylindrical control boxes can be designed using simple pressure vessel theory. However, for structures like the main body of the proposed Hydrocopter, one would need to use numerical procedures like finite element analysis. A detailed code would not have to be developed. The actual design could be accomplished by using commercial software packages like ANSYS or ALGOR.

The hull form plays an important part in the stability and manoeuvrability at different speeds of an underwater vehicle. The hydrodynamic form besides determining propulsion energy required may also impose limitations on

vehicle access, launch and recovery and maintenance. Further information may be found in *AUV Design Info Page*. <http://www.ise.bc.ca/WADEhullform.html>.

Additional factors affecting the hull form include minimizing flow separation especially for efficient propulsion at the tail and minimization of overall vehicle drag. Vehicle drag consists of friction drag and form drag. Friction drag is a function of speed and the exposed surface area which will be minimized by using small hulls with less surface area. Longer, more slender shapes are better for minimizing flow separation which minimizes form drag.

The Carmichael hull developed in the 1970's represents the best option to reduce drag. The flow over the hull is laminar (Figure 3.3) in nature and thus the skin friction drag is much lower than in a turbulent boundary layer where the fluid particles move more erratically resulting in higher shear stresses between layers and the surface. The surface of the hull must be smooth. The limitation of this



Figure 3.3 Example of Laminar Flow Hull

type of hull is that lengthening or shortening of the hull is extremely difficult, and therefore modular expansion of the vehicle is not possible.

The 'torpedo body' is a simple alternative to the laminar flow form. It has a nose cap followed by a cylindrical midsection and a tapered tail section (Figure 3.4).

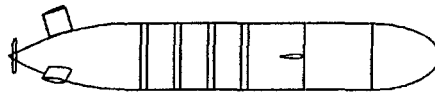


Figure 3.4 Example of Torpedo Body Hull

Although this type of configuration can have up to 30 percent more drag compared to the laminar type, it has the advantage of being relatively insensitive to manufacturing imperfections, has greater capacity for carrying payload and power source, and allows extension or contraction of the middle cylindrical section.

The Hydrocopter body is cylindrical in shape, and for simplicity the tail and front are sealed by circular end-caps. The main objective is to demonstrate a concept therefore this was the simplest and cheapest design option.

The material used for the body has to be light, and at the same time be able to withstand pressures at various depths below the surface. Since the range of an AUV is limited by the amount of energy and payload, aluminum or plastic or composite bodies are the choice materials.

3.6 Energy System

The Hydrocopter was designed using existing low cost enerCELL nickel cadmium batteries rated at 8 Volts. These batteries are reliable and of good performance which have been used in previous models of small submersibles. The cyclic life of these batteries is comparable to those of lead acid batteries, which can also be used in this application. The advantage of nickel cadmium batteries is that cold temperatures do not affect their performance, as is the case with lead acid batteries. Silver - zinc batteries have been used on commercial applications of AUV's such as the Explorer developed by ISE Limited. These are available off the shelf, but due to the high cost and low endurance are being replaced by longer lasting Lithium Ion and Lithium Polymer batteries.

3.7 Buoyancy

Buoyancy is an important factor in the design of an AUV. If the vessel is too positively buoyant, it will float on the surface whereas if the AUV is negatively buoyant, the AUV may sink if there is a system malfunction. Buoyancy in a submerged vehicle may be controlled by using a dynamic system that can compensate for pressure at any depth, through a complex system of valves, ballast tanks, and compressed air. The drawback of such a system is that it requires a large amount of space and may not be reliable in maintaining proper buoyancy. The Hydrocopter was fitted with a circular ring outside the hull with a weight that made the model neutrally buoyant. This ring can be manually adjusted to alter the center of gravity of the Hydrocopter both vertically and laterally.

CHAPTER 4

SIMULINK DYNAMICS SIMULATION

SIMULINK under MATLAB has a feature allowing a complete 3D simulation of the Hydrocopter motion. However, it requires many cross coupling parameters that would be extremely difficult if not impossible to calculate. A much simpler simulation was used. The assumption was made that heave of the vehicle was a function of surge speed and pitch only. Because of the fin, the pitch of the model was controlled by surge speed.

The overall block diagram can be seen in Figure 4.1. In the subblocks Newton's Second Law was used for each Degree of Freedom or DOF. A first order model was used for the drives. PID was used to generate drive signals. The subblock labelled CONTROL takes in the desired pitch angle and compares it with the pitch angle from the PITCH dynamics subblock. Output from the CONTROL subblock is a command surge speed. This goes into the SURGE subblock to give surge. Surge feeds into the PITCH subblock and influences pitch because of the fin. Pitch and surge feed into the HEAVE subblock. It calculates the vertical component of the forward motion of the vehicle. This is

integrated to give the heave or z location of the vehicle. Pitch, surge and yaw feed into the XY subblock. This calculates the horizontal component of the forward motion of the vehicle and converts it into x and y components. These are integrated to give the x and y locations of the vehicle. The WORKSPACE subblocks send the xyz coordinates out to MATLAB proper where they are plotted using the plot3 function.

Figure 4.2 shows the CONTROL subblock. Input #1 is the desired pitch angle while input #2 is the actual pitch angle. The pitch angle error is integrated to give the command surge which is output #1. Figure 4.3 shows the SURGE subblock. As can be seen this has the standard feedback control form. Input #1 is the command surge. This is compared with the actual surge. A control signal based on surge error feeds into the propeller drive dynamics which in turns feeds into the surge dynamics to give surge which is output#1. Figure 4.4 shows the PITCH subblock. As can be seen in the diagram this is open loop, Input #1 is surge. The fin generates a pitch moment based on surge. This counterbalances a pitch moment due to the center of gravity location relative to the center of buoyancy. These two moments feed into pitch dynamics which gives pitch which is output #1. Figure 4.5 shows the YAW

subblock. As can be seen this has the standard feedback form. Input#1 is the desired yaw angle. This is compared with the actual yaw angle. A control signal based on yaw error feeds into propeller dynamics which in turn feeds into yaw dynamics to give yaw, which is output #1. Figure 4.6 shows the HEAVE subblock, Input #1 is surge while input #2 is pitch. These are used to get the vertical motion of the vehicle. Integration of this gives its vertical locations. Figure 4.7 shows the XY subblock. Input #1 is surge and input #2 is pitch while input #3 is yaw. Surge and pitch are used to achieve the horizontal motion of the vehicle. Yaw is then used to break this up into x and y components. Integration of this gives the x and y locations of the vehicle.

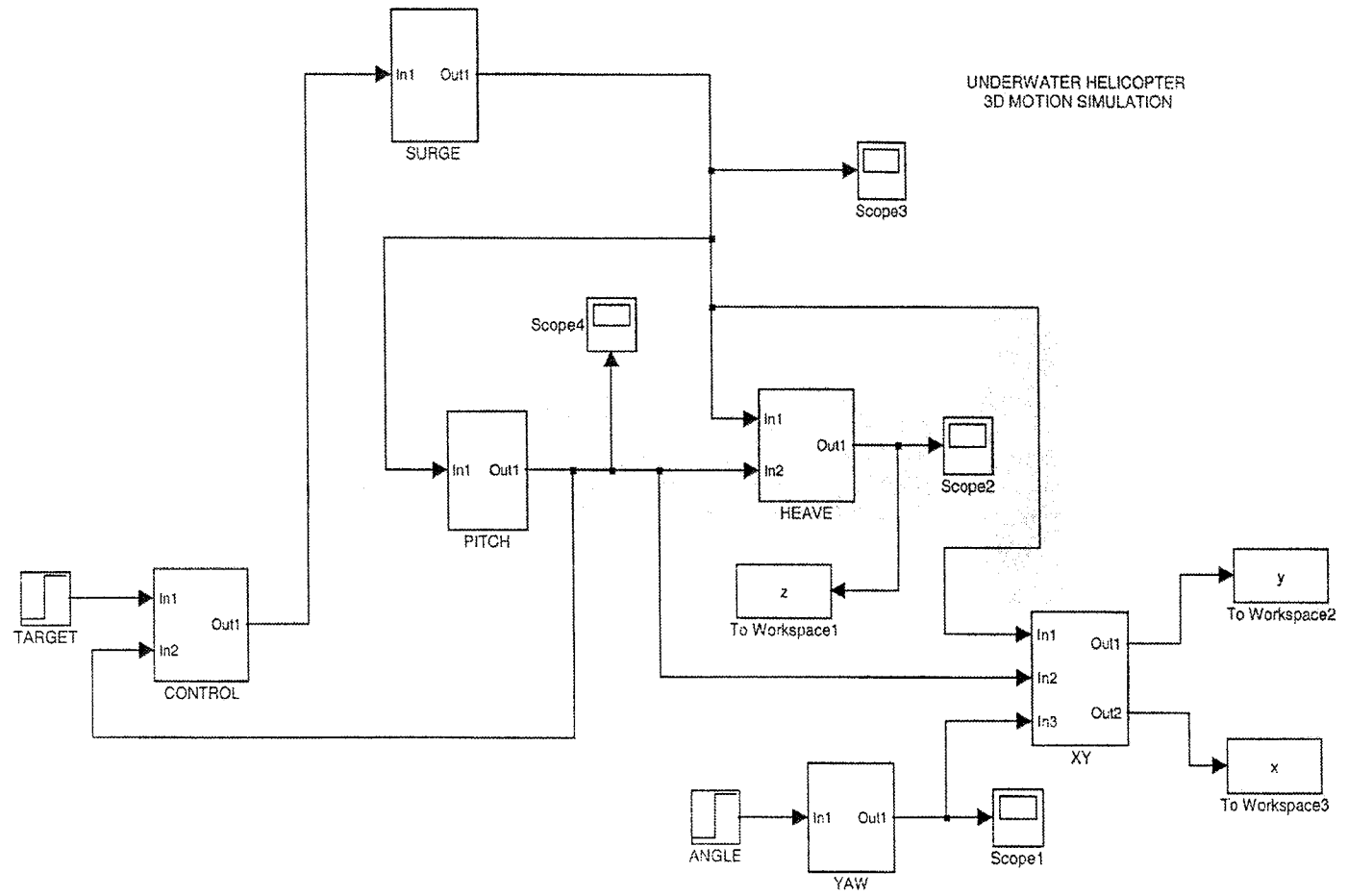


Figure 4.1 Overall Block Diagram

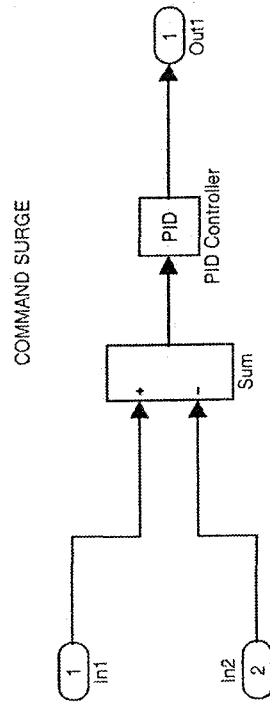


Figure 4.2 Control Subblock

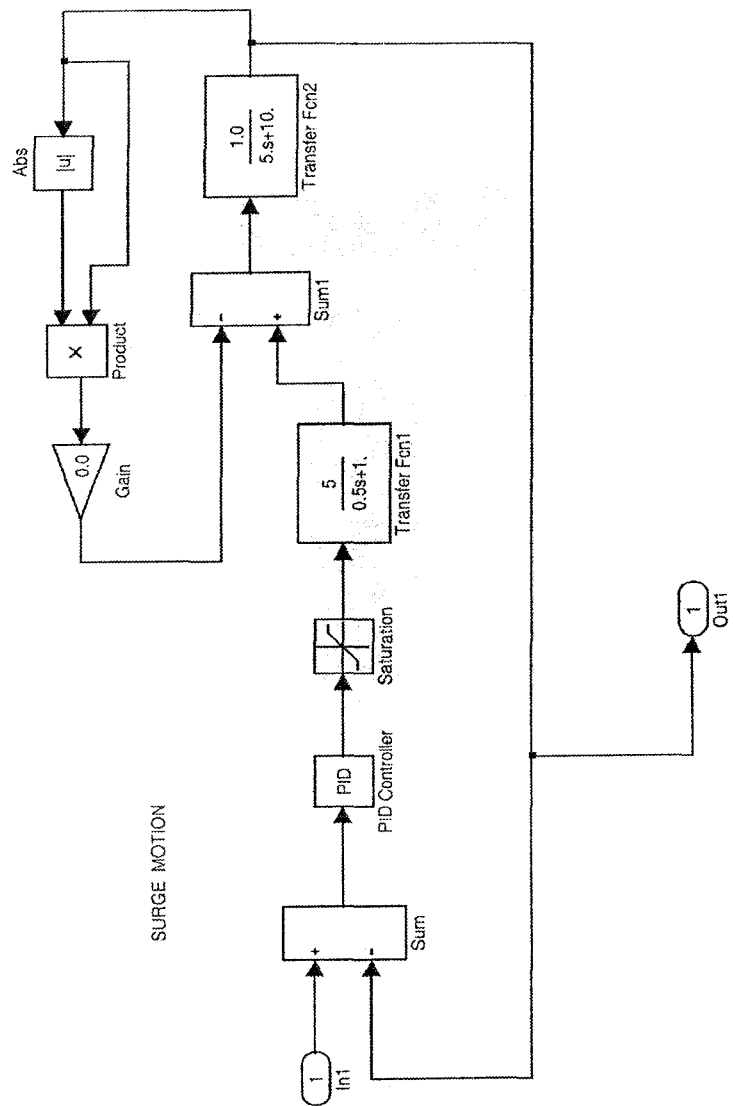


Figure 4.3 Surge Subblock

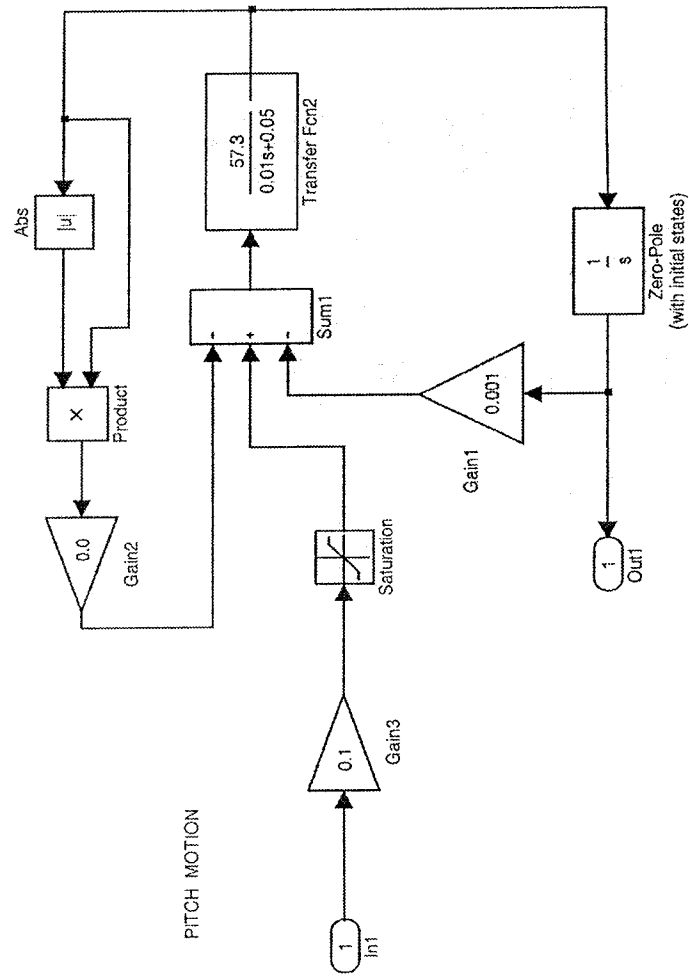


Figure 4.4 Pitch Subblock

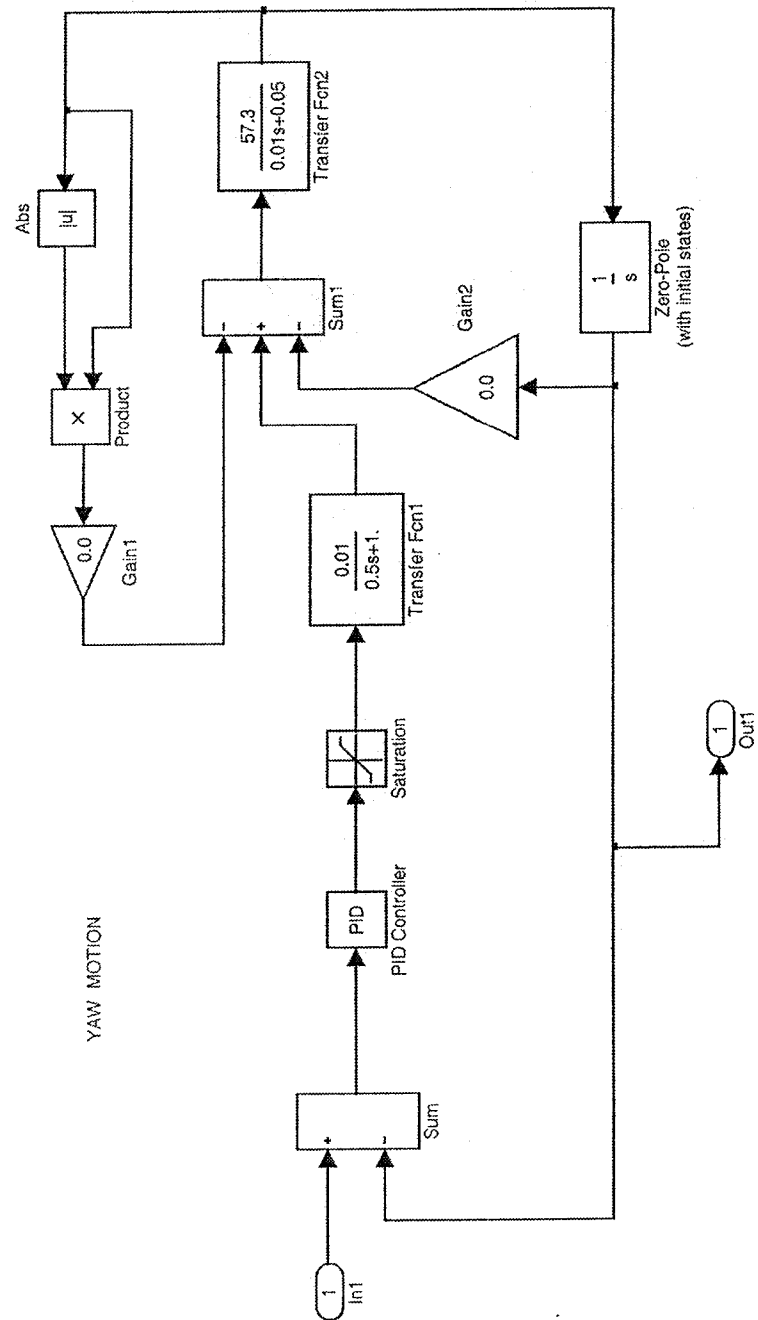


Figure 4.5 Yaw Subblock

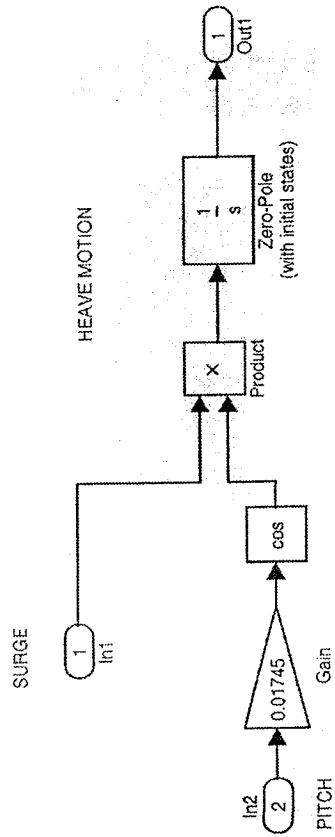


Figure 4.6 Heave Subblock

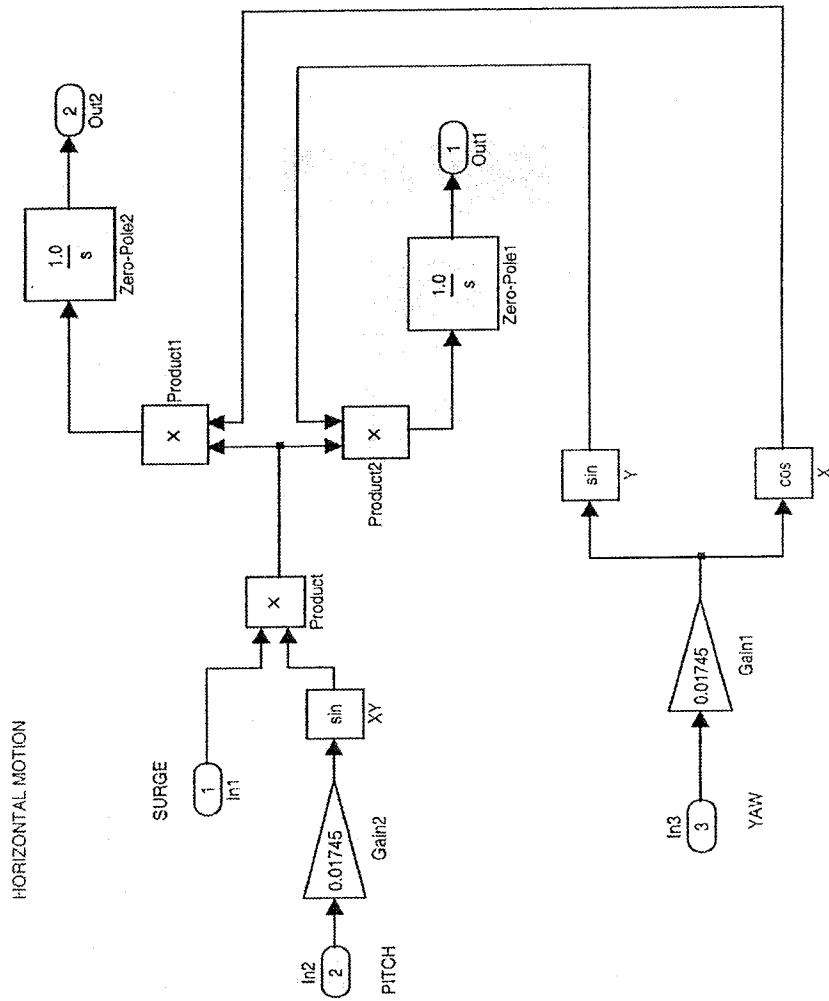


Figure 4.7 XY Subblock

CHAPTER 5

HYDROCOPTER MODEL

5.1 Design Criteria

The Hydrocopter model was designed by applying hydrostatic and hydrodynamic principles. Its design criteria included:

1. Model weight must equal model buoyancy.
2. The model centre of gravity C_G must be below the model centre buoyancy C_B .
3. The model shape must have low drag.
4. The model must be highly maneuverable.
5. The model must be dynamically stable.

5.2 Hydrocopter Model Components

The main components of the model Hydrocopter are its: frame, propellers, power system, control system, and manually adjustable fins. Figure 1.1 shows the complete model. Specification sheets for various components are given in Appendix B.

5.2.1 Model Body

A PVC plastic tube was used as the model body. It was sized to fit other components like propellers and motors. It housed all of the electronic components such as the controller and batteries. The tube was closed by two plastic end caps which were held into place by hook and claw clamps. Two plastic motor mounts were attached to the tube. A rod attached to each motor passed through a simple tube stuffing box in the motor mounts. A propeller was attached to each of these rods.

5.2.2 Energy Storage System

Two 8VDC batteries in series were used to provide power to each of the motors. A separate 9 VDC battery was used to provide 5VDC logic for the electric circuits. This was attached to two separate 5VDC regulators. One supplied power to the controller and the other supplied power to the sensors. This arrangement was used to ensure that the controller was not disturbed by sensor fluctuations.

5.2.3 Propulsion System

Two propellers were used to move the model forward in surge and rotate in yaw. A fixed fin at the rear of the model was used to provide pitch up or down. Together with surge this caused the model to heave.

5.2.4 Sensors

An OMEGA PX40 pressure sensor was used to detect the depth of the model below the water surface. It was powered by 5VDC and had a 0.5VDC to 4.5 VDC output range. A photo of the sensor is shown in Figure 5.1. An inclinometer could have been used to detect the pitch of the model, however an IC SENSORS Model 3145-002 accelerometer was used as it was readily available and had a good output range. It was powered by 5 Volt DC, a photo of this sensor is shown in Figure 5.2. A magnetic digital compass could have been used to detect yaw, however this was not available. For the proof of concept test program all that was required for the model to be able to move along an arbitrary 3D trajectory so the exact yaw orientation was not critical.

5.2.5 Control System

The PIC16F873 controller was used to control the motion of the model. It took in signals from the pressure sensor and the accelerometer and gave out pulse width modulation signals to two H Bridge Drivers which ran the two motors. A schematic of the control circuit is shown in Figure 5.3. Two wires connect each bridge to the controller. One is the pulse width modulation wire and the other is a direction wire which makes the motor go forward or reverse.

5.2.6 Control Code

The following is a brief description of the major parts of the control code which were used to control the model and in the following pages are the code for the Hydrocopter Motion Control:

The section of the code labeled "SET PINS and PWMS" activates the PWM channels on the PIC and its analog input channels. The section labeled "READ SENSOR OFFSETS" reads the offset or bias values of the depth and pitch sensors. The section labeled "START MISSION" uses the depth sensor to sense when the model has been put in the

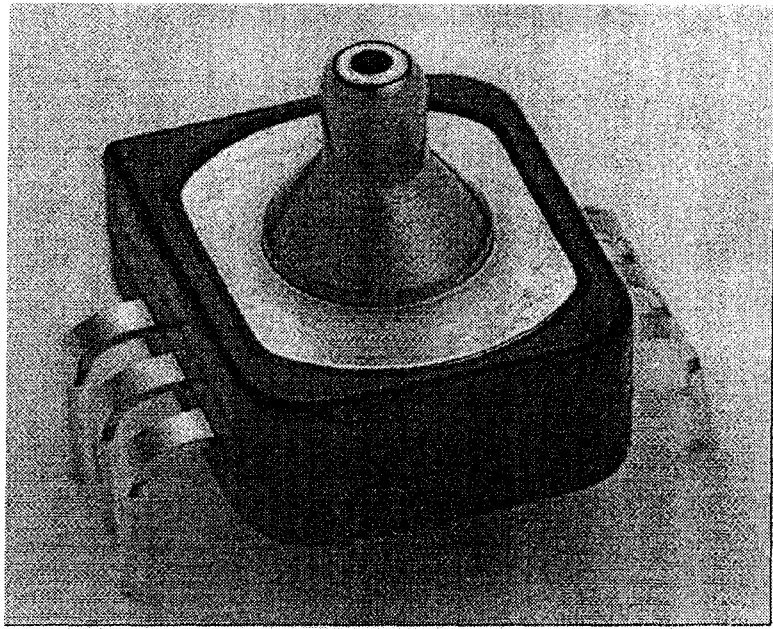


Figure 5.1 Omega Pressure Sensor

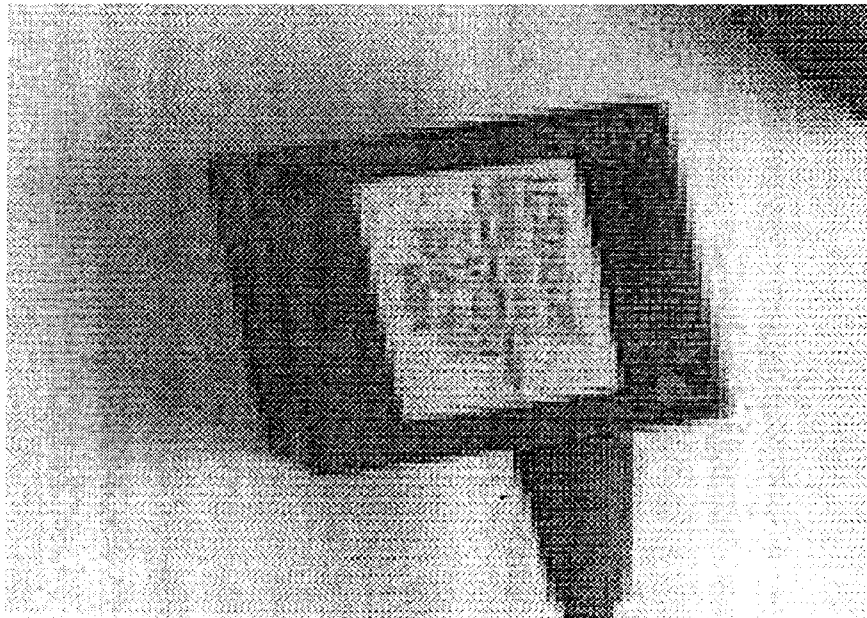


Figure 5.2 IC Sensors Accelerometer

water and starts the test run. The section labeled "DEPTH CONTROL" reads the depth sensor and generates a PWM drive signal based on depth error. The section labeled "PITCH CONTROL" reads the pitch sensor and generates a command surge PWM signal based on pitch error. A sensor pin is activated by the statement `set_adc_channel(#)`. The `read_adc()` statement reads it. A PWM drive signal is generated by `set_pwm#_duty(#)`. The statements which control the direction of propeller rotation are: `output_high(#)` or `output_low (#)`.

A flow chart for the code is given in Figure 5.4.

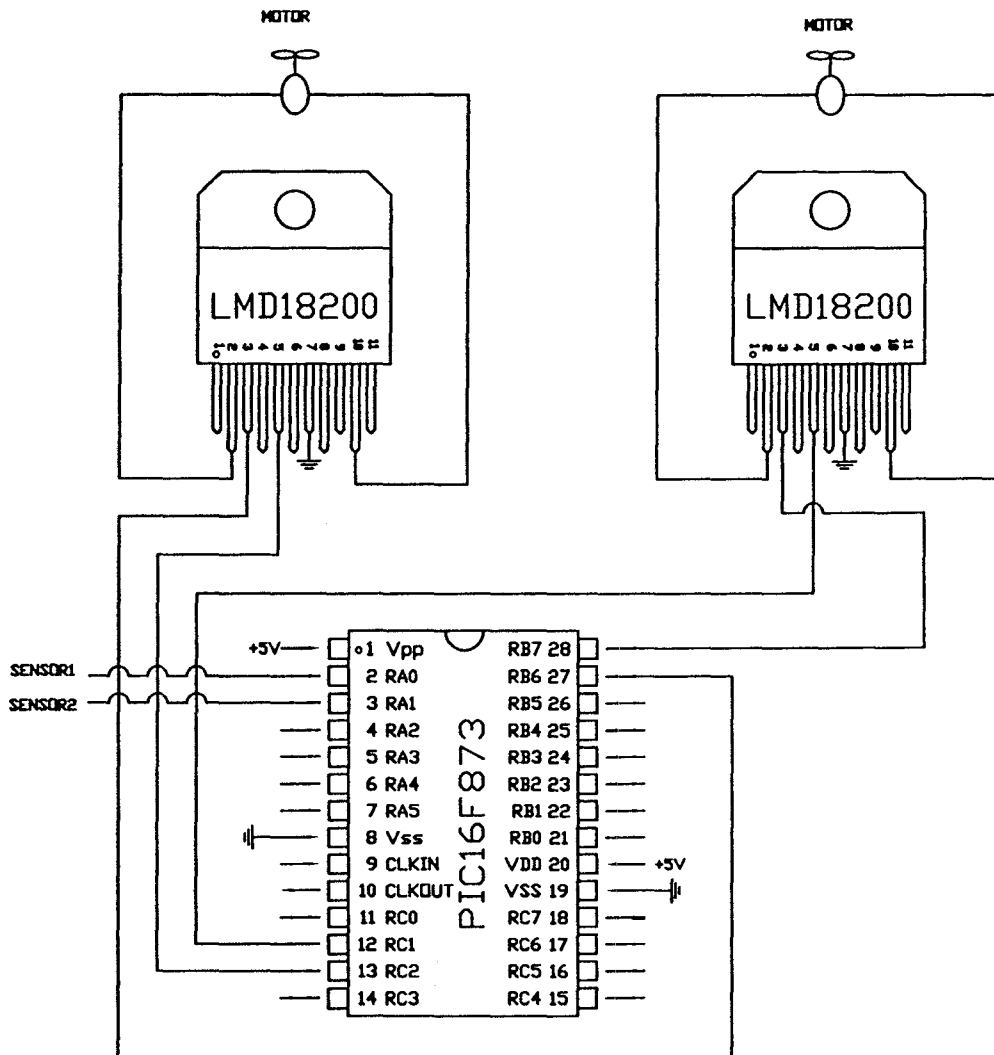


Figure 5.3 Control Circuit

```

/*****/

/*  HYDROCOPTER MOTION CONTROL  */

/*****/

/*  HEADER FILES  */
#include <16f873.h>
#include HS,NOWDT,NOPROTECT
#include PIC16F873 ADC=10
#include <stdlib.h>

/*****/

/*  DECLARE VARIABLE TYPES  */
float pitch,offset;
float heave,angle;
float depth,bias;
float error,wrong;
float signal,data;
float size,band;
float gp,sum;
int8 one,two;

/*****/

/*  MAIN LOOP  */

void main()

{
/*****/

/*  SET PINS & PWMS  */
set_tris_b(0x00);
setup_adc_ports(ALL_ANALOG);
setup_adc(ADC_CLOCK_INTERNAL);
setup_timer_2(T2_DIV_BY_1,254,1);
setup_ccp1(CCP_PWM);
set_pwm1_duty(0);
setup_ccp2(CCP_PWM);
set_pwm2_duty(0);

/*****/

```

```

/*      READ SENSOR OFFSETS      */
    set_adc_channel(0);
    delay_us(21);
    bias=read_adc();
    delay_ms(5000);
    set_adc_channel(1);
    delay_us(21);
    offset=read_adc();
    delay_ms(5000);

/*****/

/*      PARAMETERS      */
    delay_ms(5000);
    heave=88; angle=500;
    sum=25.0; gp=0.5;

/*****/

/*      START MISSION      */
    set_adc_channel(0);
    while(TRUE)
    data=read_adc();
    delay_ms(100);
    depth=data-bias;
    if(depth>11)
    {break;}}

/*****/
/*      CONTROL LOOP      */

    while(TRUE)
    {

/*****/
/*      DEPTH CONTROL      */
    set_adc_channel(0);
    delay_us(21);
    data=read_adc();
    delay_ms(100);
    depth=data-bias;
    error=heave-depth;
    signal=gp*error;
    size=abs(signal);

```

```

        if(size>100.0)
            {size=100;}
        one=size;two=size;
        if(error>+band){
            set_pwm1_duty(one);
            set_pwm2_duty(two);
            output_low(PIN_B6);
            output_low(PIN_B7);}
        if(error<-band){
            set_pwm1_duty(one);
            set_pwm2_duty(two);
            output_high(PIN_B6);
            output_high(PIN_B7);}

/*****
/*          PITCH CONTROL          */
        if(abs(error)<band){
            set_adc_channel(1);
            delay_us(21);
            data=read_adc();
            delay_ms(100);
            pitch=data-offset;
            wrong=angle-pitch;
            if(wrong>0.0) {sum=sum+5;}
            if(wrong<0.0) {sum=sum-5;}
            if(sum>200.0) {sum=200.0;}
            one=sum+10;two=sum-10;
            set_pwm1_duty(one);
            set_pwm2_duty(two);
            output_high(PIN_B6);
            output_high(PIN_B7);}

/*****/

    }

}

```

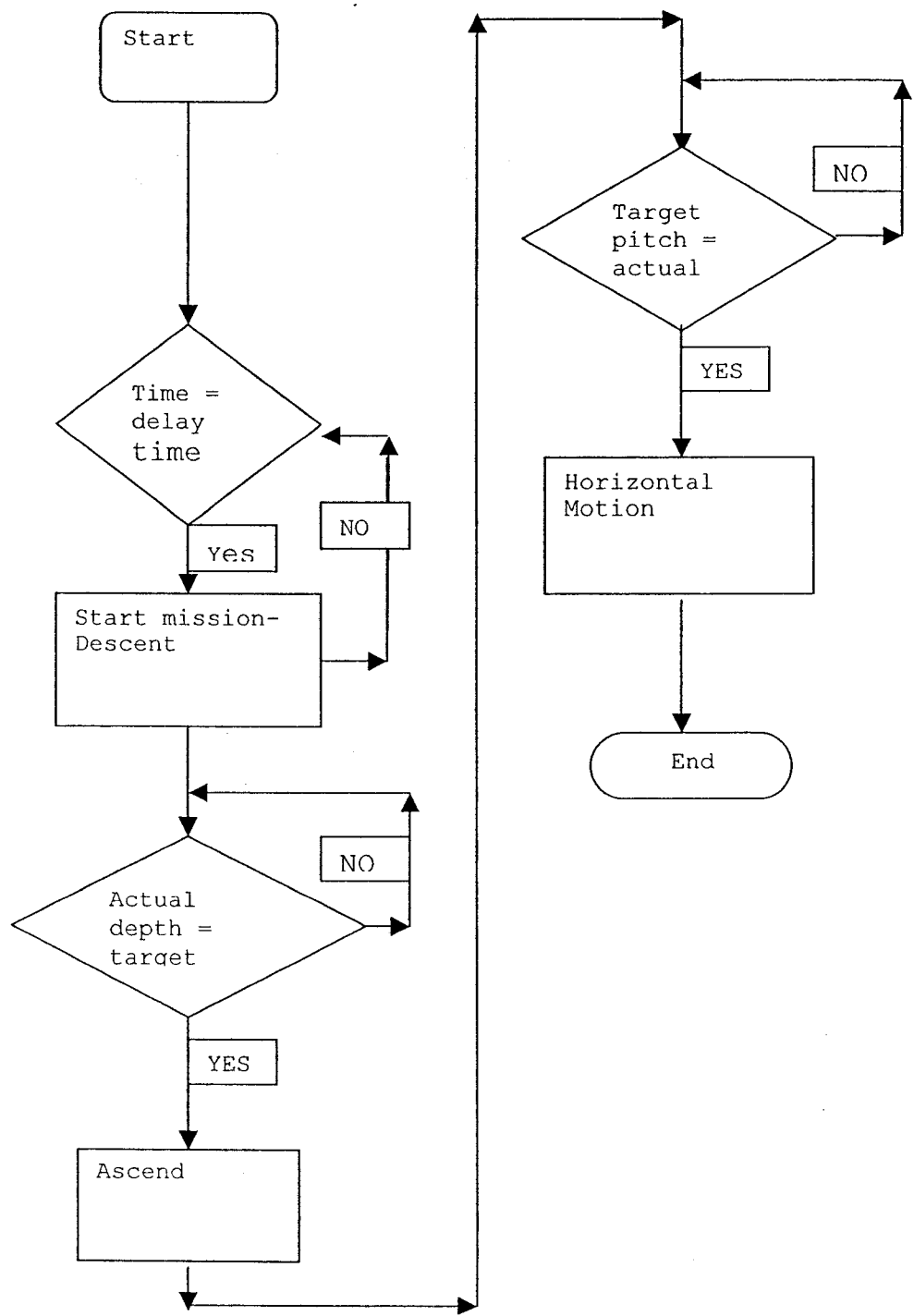


Figure 5.4 Control chart

CHAPTER 6

RESULTS OF SIMULATION AND TESTS

The SIMULINK simulation was first used to help design the model Hydrocopter. Once the model had been constructed, calculations and experiments were used to obtain more accurate estimates of the parameters in the model, such as inertias and drag factors. This work is described in Appendix A.A computer animation of the Hydrocopter trajectories was also constructed using Autodesk Inventor software. The animation was produced after constructing a 3D drawing of the model.

Figure 6.1 shows a simulation plot for a case where the model was at a certain depth and was commanded to fly horizontally. The plot shows the vehicle performs according to commands.

Tests were conducted in the Deep Water Tank at MUN, this 4m x 4m x 8m tank is shown in the photo in Figure 6.2. Two sets of tests were conducted. In the first set, the model in a vertical orientation was commanded to hover at a preset depth below the water surface. In the second set, the model was commanded to fly horizontally starting from a vertical orientation. Due to the small size of the tank,

for the second set of tests, the props rotated at different speeds which caused the model to fly in an approximately circular orbit. This usually prevented the model from running into the walls of the tank.

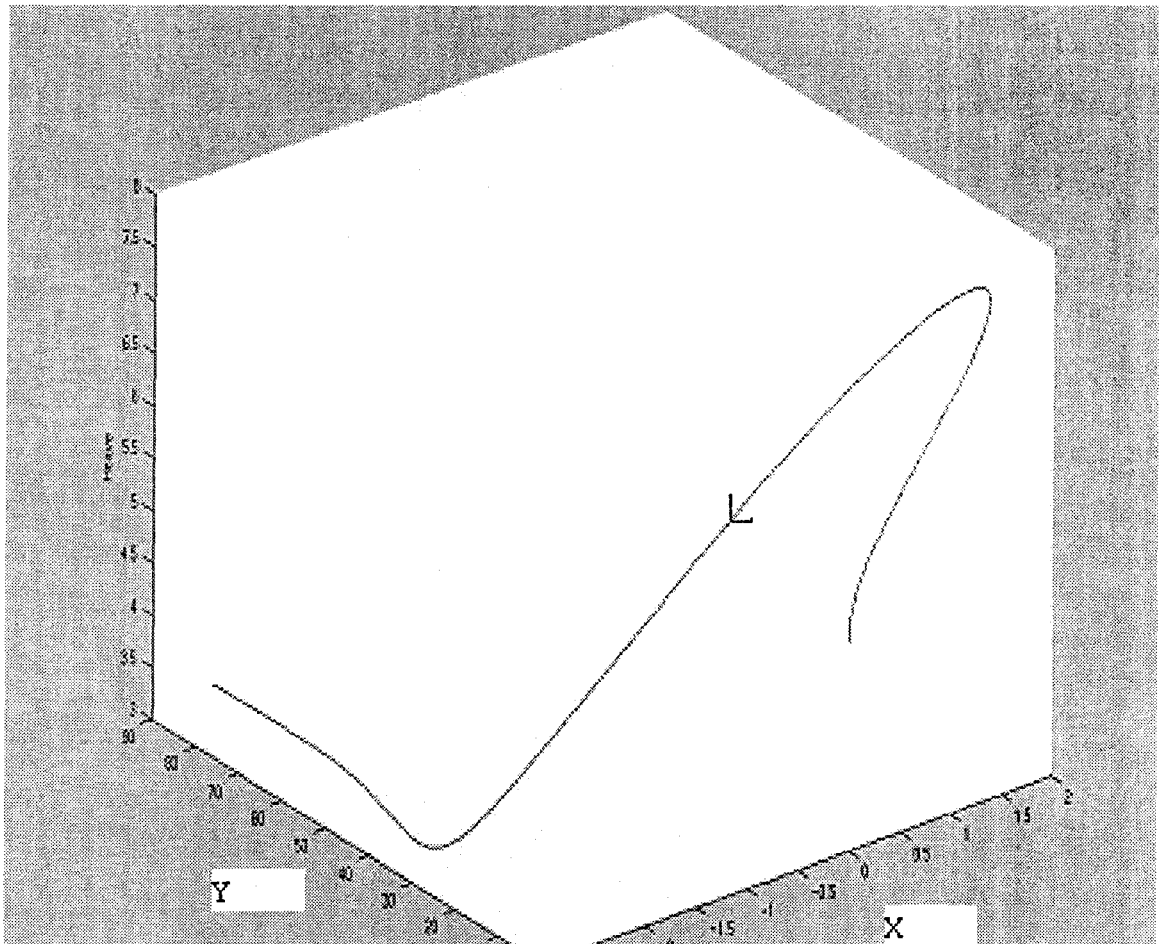


Figure 6.1 3D Plot of Hydrocopter Simulation

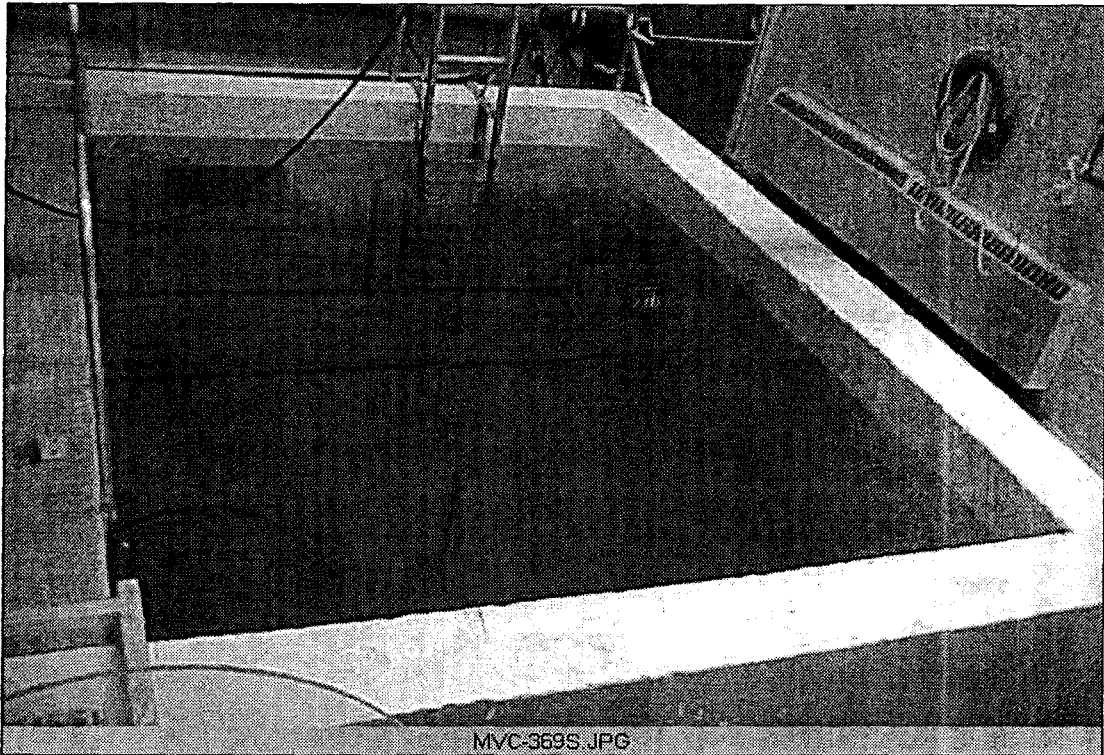


Figure 6.2 Test Tank

Only photographic and video records were made of the tests, however tests were usually witnessed by two people. Wires could have been attached to the model to record sensor data but these would have interfered with the motion of the model. A thin neutrally buoyant plastic rope was attached for most tests, unfortunately this rope sometimes became entangled with the props. When this happened the motors would stall and overheat which sometimes caused the H bridges to burn out.

Figure 6.3 shows a photo of a computer animation model in vertical motion. Figure 6.4 shows a photo from a Deep

Tank test where the model was commanded to go to a certain depth and hover while in a vertical orientation. This test was performed many times and was very repeatable. It successfully proved that the model was able to hover at a set depth.

Figure 6.5 shows a photo of a computer animation model in horizontal motion. Figure 6.6 shows photos from a Deep Tank test where the model was commanded to fly horizontally in a circular orbit after going down to a pre-set depth. This set of tests once again proved that the vehicle can move along a 3D trajectory at high speed.

During the second set of tests the model sometimes moved close to the tank walls and had to be nudged away by the rope. In one instance, the model actually did a back flip much like a diver diving backwards from a diving board. Following the flip it went back into the approximately circular orbit! It had been expected that many trials would have had to be conducted during the set of tests to get the model to move along a circular orbit. Surprisingly, the model went into a circular orbit the first time it was attempted!

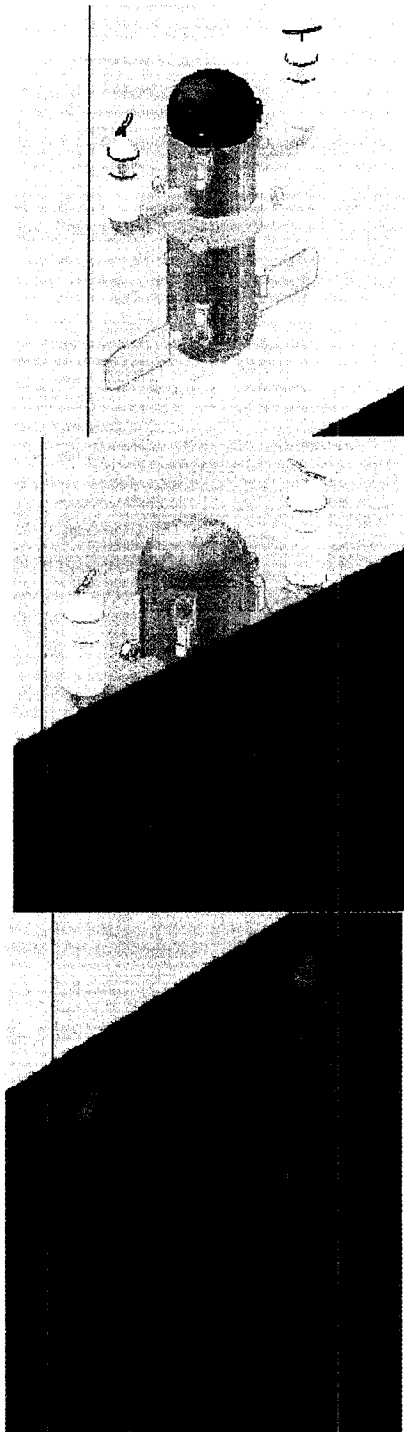


Figure 6.3 Computer Animation of Vertical Motion

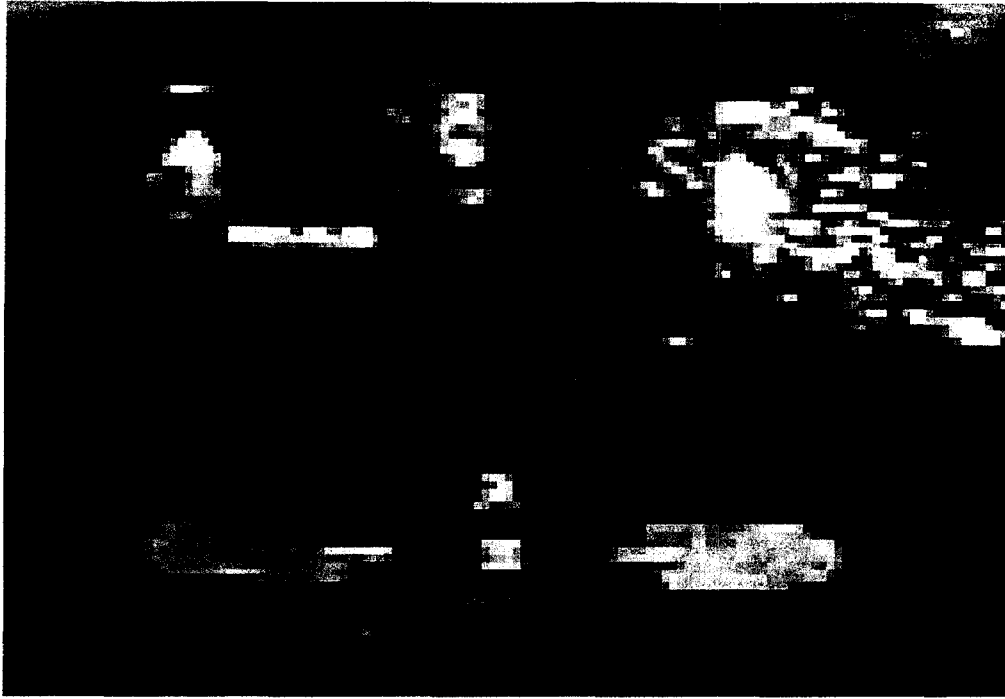


Figure 6.4 Vertical Motion Test in Tank

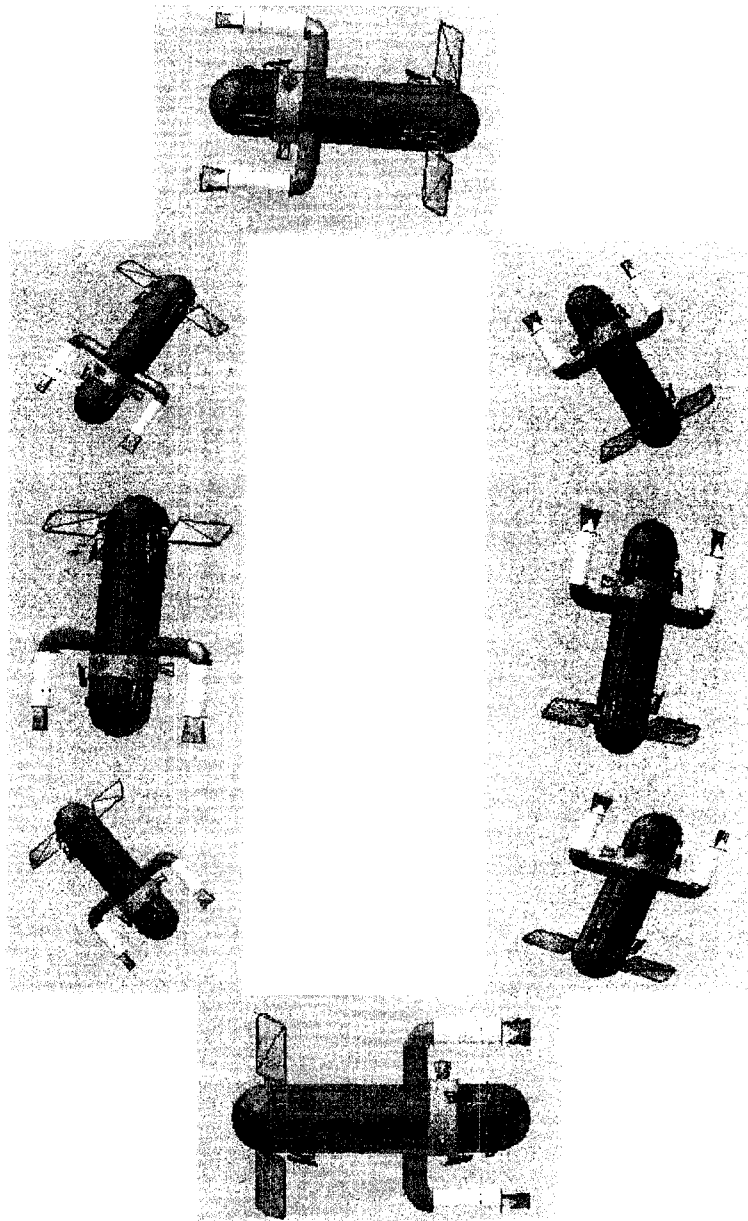


Figure 6.5 Computer Animation of Horizontal Motion of the Hydrocopter

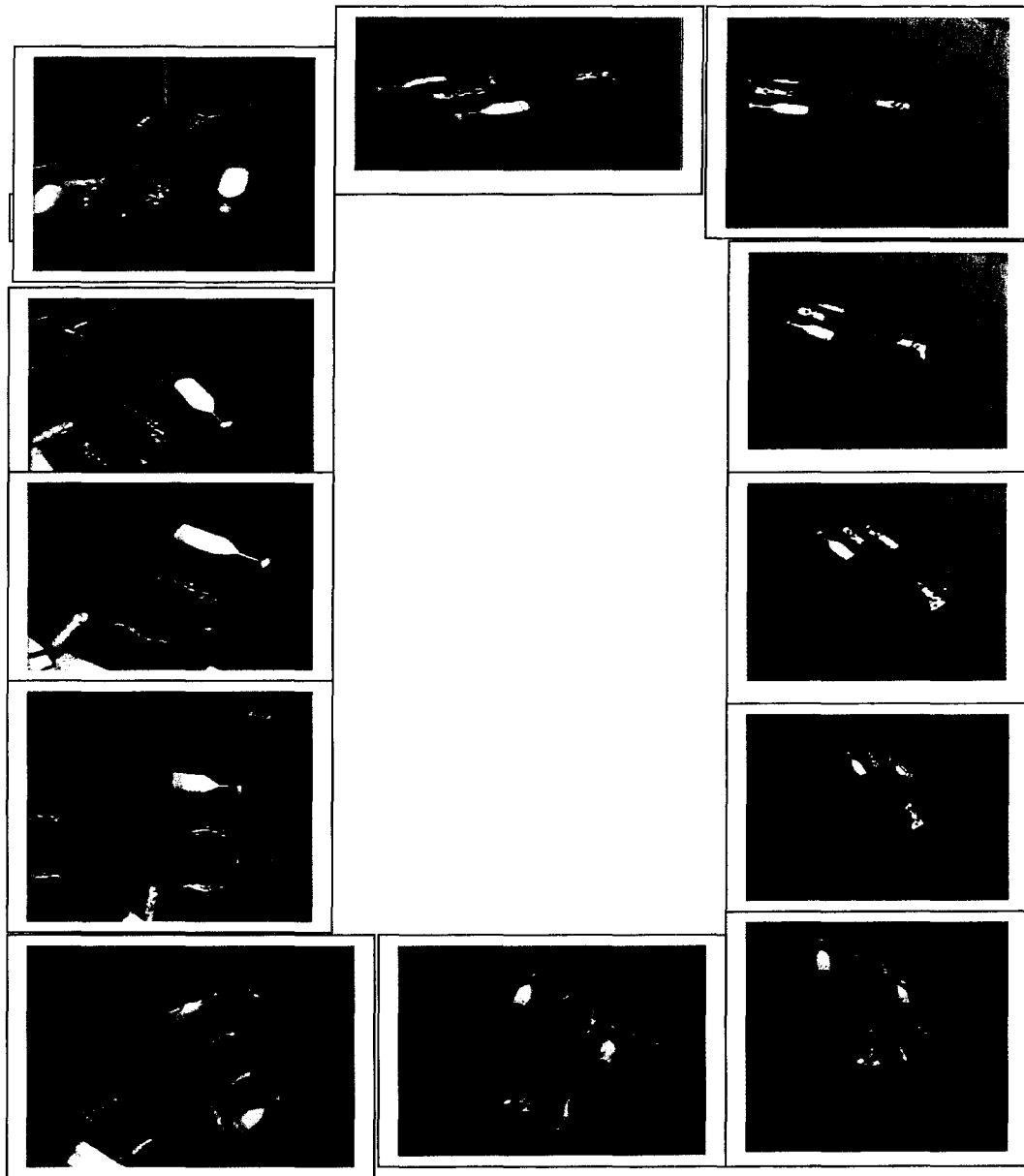


Fig 6.6 Robot in Horizontal Motion during Test

CHAPTER 7

CONCLUSIONS AND FUTURE WORK

The tank tests at MUN show that the model Hydrocopter can move at a high speed along any 3D trajectory underwater. The simulation responses confirm this.

In the future, a more realistic model needs to be constructed, meaning better drives and sensors. The model developed in this thesis used whatever components were available. The new model would use an adjustable fin and would resemble the prototype in every detail.

After the new model has been tested, a prototype should be constructed. This will make use of design for manufacture and assembly (DFMA) concepts. A fail safe system would be needed in the prototype. This could be a simple float or a drop weight.

The model developed in this thesis is basically an electromechanical system. Labs could be developed around this model for mechatronic and controls courses at MUN.

REFERENCES

- [1] Allmendinger Eugene E (1990). Submersible Vehicle Systems. Society of Naval Architects and Marine Engineers Design, Society of Naval Architects and Marine Engineers.
- [2] Anderson Poul and Breslin John P. Hydrodynamics of ship propellers., Cambridge Ocean Technology Series 3. Cambridge University Press 1994
- [3] Animatics . Motor success checklist.
www.animatics.com/download/sm_checklist.pdf.
- [4] AUV Design Info Page.
<http://www.ise.bc.ca/WADEhullform.html>
- [5] Boothroyd 1994 Product design for manufacturing and assembly. Computer Aided Design, 26. 505 - 519.
- [6] Brooks Rodney A. ,Control System for a mobile robot. Ref IEEE. Journal of Robotics and automation. Vol RA2 Mar 1986
- [7] Butler Bruce and Hertog Vinceden. Theseus: A cable laying AUV. <http://www.ise.bc.ca/auv1003.html>
- [8] Butler Bruce, Pope Allen, Ferguson James and Verral Ronald I., Theseus AUV-Two record breaking missions
- [9] C-Scout- Canadian Self Contained Off the Shelf Underwater Testbed -
<http://www.engr.mun.ca/~cscout/multimedia.htm>
- [10] Capson David W. and Schuurman Derek C. "Robust Direct Visual Servo Using Network - Synchronised Cameras. IEEE Transactions on Robotics and Automation. Volume 20, No. 2. April 2004
- [11] Eddy David and Jackson Eric. Design and Implementation Methodology for Autonomous Robot Control Systems. ISE Ltd. <http://www.ise.bc.ca/robotics-paper.html>

- [12] ESI Electronic surplus Inc. Accelerometer -2 to +2G Signal. <http://www.electronicssurplus.com>
- [13] Finnemore John E; Franzine Joseph B., Fluid Mechanics with Engineering Applications. Tenth Edition.2002 McGraw Hill
- [14] Franklin, Powell and Emami-Naeini., Feedback control of dynamic systems. Fourth edition
- [15] Govil K. Manish and Magrab Edward B., Implementing production concerns in conceptual product design. Int. Journal of Production. 2000. Vol 38, No 16,383-3843
- [16] Harvald SV. AA., Resistance and Propulsion of ships. A Wiley-Interscience Publication. John Wiley and Sons. 1983
- [17] Hinchey M.(2004): Automatic Control Engineering, Bookstore Notes, Memorial University of Newfoundland.
- [18] International Submarine Engineering Limited.Research and development <http://www.ise.bc.ca>
- [19] Jani R. and Hinchey M. Development of a hydrocopter. Proceedings of NECEC 2004. Oct 2004.
- [20] Jani R and Hinchey M. Development of a hydrocopter. Proceedings of IEE ICMA 2005. July 2005.
- [21] LUZ (1996).,Development of the Subsea Robot NO MAD. Doctoral thesis, Memorial University of Newfoundland: St. John's Newfoundland
- [22] Muggerridge, K.J., Hinchey, M.J. 1994. "Investigation of control strategies and development of a hydraulic actuator mechanism for accurate positioning of subsea robots", Faculty of Engineering and Applied Science, Memorial University of Newfoundland, St. John's, NL, Canada ,September 1994.
- [23] Oceaneering. Remotely operated Vehicles. <http://www.oceaneering.com>

- [24] Prandtl and Tietjens Applied Hydro-and Aeromechanics.,
Dover Publications, USA.
- [25] Peripheral Interface Controller. Data sheets.
<http://www.hotspotter.scottcressman.com/docs/16F877%20datasheet.pdf>
- [26] Reed Everett F. Lateral Vibration of Shafting .SNAME
Committee on Ship Machinery Vibrations.Propellers
shafting '94 symposium.NO. 5
- [27] Seaeye Marine- Manufacturers of electric powered ROV
systems. <http://www.seaeye.com/>
- [28] Slotine Jean- Jacques E, sliding controller design for
non- linear systems. Int. J.Control,1984,Vol.40, No.2,
421-434
- [29] Southampton Oceanography Center. Ocean Engineering
Division Autosub.
<http://www.soc.soton.ac.uk/OED/index.plp?page=vd>
- [30] Woolgar,Reeni Catherine .," Development of the subsea
robot ANNE (Autonomous Pneumatic Nautical Explorer)";
Faculty of Engineering and Applied Science;. Memorial
University of Newfoundland. Newfoundland
1999
- [31] Yoerger Dana R, Cooke John G, Slotine Jean - Jacques E.
The influence of Thruster Dynamics on underwater
Vehicle Behavior and their Incorporation Into Control
System Design. IEEE Journal of Oceanic Engineering.
Vol15.No.3, July 1990.

APPENDIX A

Estimation of Hydrocopter Parameters

ESTIMATION OF HYDROCOPTER PARAMETERS

When an underwater vehicle accelerates or decelerates, it accelerates or decelerates the surrounding water. The vehicle appears to be more massive. The inertia of the Hydrocopter for surge and heave motions consists of the basic mass of the vehicle plus some added mass. A typical value for added mass is 50% of the basic mass. The inertia of the Hydrocopter for pitch and yaw motions is equal to its mass times a radius of gyration squared. The radius of gyration for geometry with added mass is extremely difficult to determine analytically and can only be roughly estimated. A special experiment could have been setup to determine it accurately but this is beyond the scope of this thesis. Here only a rough estimate was made. The radius of gyration was taken to be one quarter the length of the vehicle.

The drag on an underwater vehicle moving at a steady speed through water can be estimated using empirical data given in texts. It could also be estimated for the Hydrocopter from a simple experiment. A small weight would be added to an otherwise neutrally buoyant Hydrocopter. It would then be allowed to free fall under gravity in a tank

of water. When the vehicle reaches a terminal speed, the drag must be equal to the extra weight:

$$\Delta W = \Delta D = C_D \rho/2 A S^2 = K S^2$$

where ΔW is the extra weight, A is the vehicle profile area and S is the terminal speed. In the experiment ΔW is set and S is measured: this allows us to calculate the drag factor K . When a vehicle is undergoing unsteady motion, this experiment is not valid because the flow around the vehicle is not steady and can be very complex. Drag on a vehicle undergoing pitch or yaw motions would be difficult to calculate analytically. Because pitch and yaw motions may not be sufficient to generate a well defined wake, the drag may be low. It would vary along the length of the vehicle. One would need to pick a characteristic radius and multiply translation drag by this radius squared. This was the approach taken here.

The Hydrocopter uses motors and propellers used on model boats having roughly the same size. Data on motors and propellers for model boats is not readily available. Another simple experiment could be used to calculate the steady characteristic of the propulsion system. A certain pwm signal from the controller could be sent to the motor drivers and the force generated by the propellers while the

vehicle is held stationary could be measured with some sort of load cell. This is known as the bullard pull test. It does not account for the motion of the vehicle. If the vehicle was allowed to move after the pwm signal was sent to the drivers, it would pick up speed until the force generated by the propellers was balanced by drag. In this case, the voltage versus thrust characteristic of the propulsion system could be measured:

$$\Delta T = C \text{ pwm}$$

where ΔT is thrust and pwm is a measure of voltage. A certain pwm produces a certain speed S which in turn implies a certain drag ΔD which in turn implies a certain thrust ΔT . The propellers do not come up to speed instantly when a pwm signal is applied to the motors. In other words, the propulsion system has a reaction time. Observations suggest that this is very low. Here it was taken to be a small fraction of the basic period of the vehicle.

On the Hydrocopter, a fin is used to induce pitch and which together with surge generates heave motion. The lift on fin when it is moving at a steady speed through water is:

$$\Delta L = C_L \rho/2 A S^2 \theta$$

where ΔL is the lift, A is the fin planform area and θ the angle of attack of the fin. This equation ignores unsteady hydrodynamics and 3D phenomena associated with vortex generation to the fin tips. The lift coefficient C_L from steady foil theory is 2π . One could perform a simple experiment to get a more accurate value of C_L . One would set S and θ and measure ΔL . This would allow us to calculate C_L . The lift force on the fin has a moment arm about the CG of the vehicle and generates a pitch moment. When the vehicle is flying at a certain pitch angle, this moment counteracts the moment due to the distance between the center of gravity (CG) and the center of buoyancy (CB).

APPENDIX B

Specification Sheets for Various Components

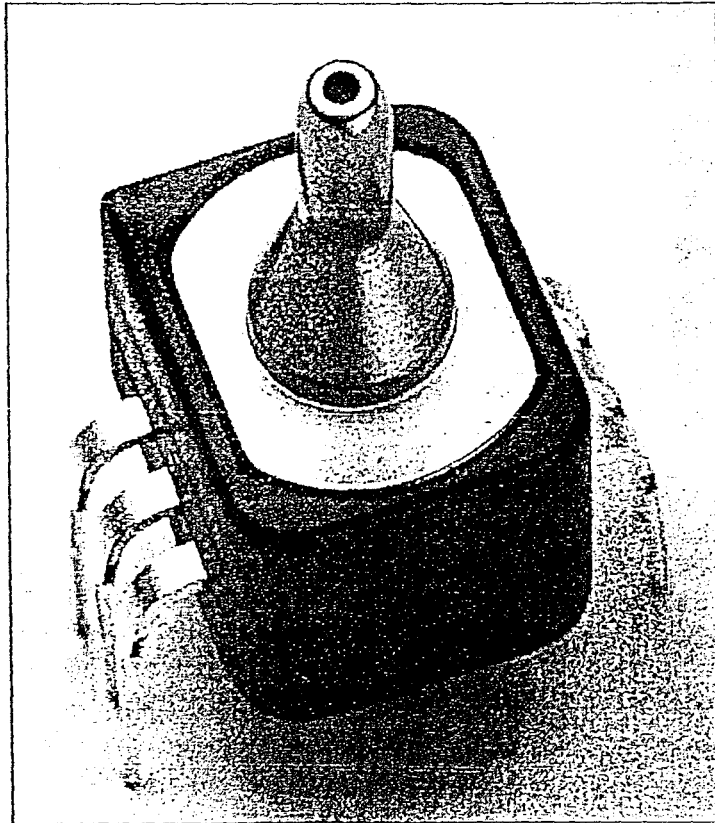
omega.ca™

Your One-Stop Source for Process Measurement and Control!

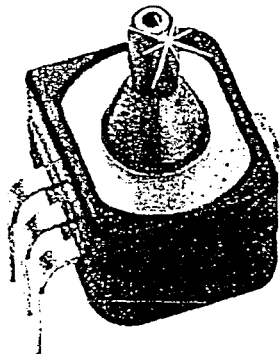


PX40

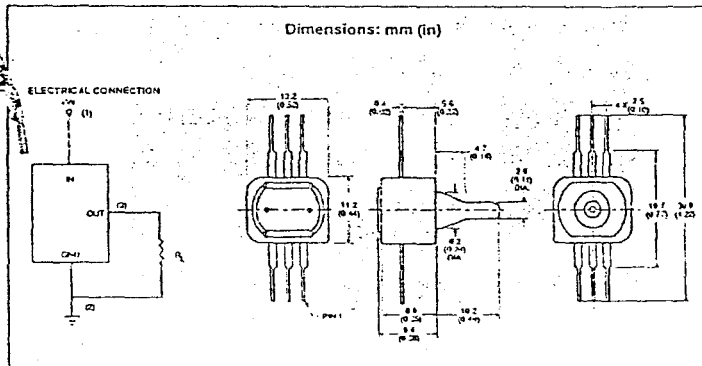
Miniature Voltage Output Pressure Sensors, Fully Temperature Compensated



MINIATURE VOLTAGE OUTPUT PRESSURE SENSORS FULLY TEMPERATURE COMPENSATED



PX40-15G5V, S60, shown much larger than actual size.



MILLIVOLT OUTPUT
PRESSURE TRANSDUCERS
B

\$60
All Models



- ✓ Smallest Amplified Package
- ✓ Small Light Weight Package
- ✓ Fully Signal Conditioned
- ✓ Temperature Compensated
- ✓ Port Designed for O-ring Interface
- ✓ Excellent Media Compatibility
- ✓ Wet or Dry Industrial Applications

Typical Applications

- ✓ Laboratory Equipment
- ✓ Electronic Brake Systems
- ✓ Engine Oil Level
- ✓ Transmission Fluid Level
- ✓ Air Conditioning Systems
- ✓ Industrial Fluid Level

SPECIFICATIONS

Excitation: 5 Vdc @ 10 mA
 Output Source Current: 0.5 mA max
 Output Sink Current: 1.0 mA max
 Hysteresis & Repeatability: 0.15% FS
 Span:
 ±50 mmHg 4.00 Vdc Typ
 0-15 4.00 ±0.11 Vdc
 0-100 4.00 ±0.09 Vdc
 0-150 4.00 ±0.07 Vdc
 0-250 4.00 ±0.07 Vdc
 Null:
 ±50 mmHg 2.50 ±0.05 Vdc
 0-15 0.50 ±0.11 Vdc
 0-100 0.50 ±0.04 Vdc
 0-150 0.50 ±0.04 Vdc
 0-250 0.50 ±0.04 Vdc

Operating Temp.:
 -45 to 125°C (-49 to 257°F)
 Compensated Temp.:
 0 to 70°C (32 to 158°F);
 (0 to 50°C 4 inH₂O)
 Overpressure:
 ±50 mmHg ±170 mmHg
 0-15 45 psi
 0-100 200 psi
 0-150 300 psi
 0-250 500 psi
 Response Time: 1 ms
 Gage Type: Silicon
 Media Compatibility: Limited to those media which will not attack invar, copper, silicon, stainless steel, glass and solder: i.e. air, water, refrigerants, engine fuel
 Weight: 0.18 oz (5 g)

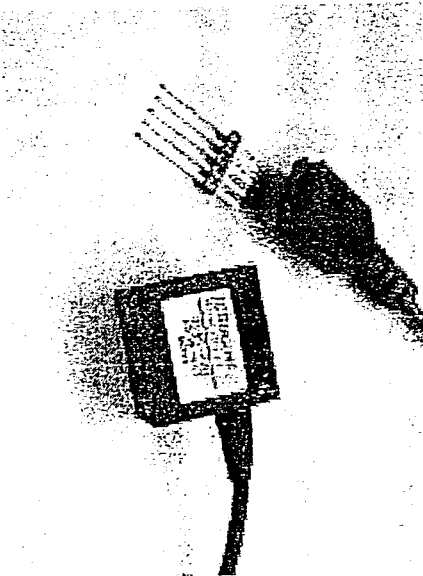
MOST POPULAR MODELS HIGHLIGHTED!

To Order: (Specify Model Number)				
GAGE MODELS (One Part)				
RANGE	MODEL NO.	PRICE	OUTPUT	COMPATIBLE METERS
±50 mmHg	PX40-50BHG5V	\$60	20.8 mV	DP24-E, DP25-E, DP41-E
0-15 psi	PX40-15G5V	60	16.6	DP24-E, DP25-E, DP41-E
0-30 psi	PX40-030G5V	60	75	DP24-E, DP25-E, DP41-E
0-100 psi	PX40-100G5V	60	15	DP24-E, DP25-E, DP41-E
0-150 psi	PX40-150G5V	60	50	DP24-E, DP25-E, DP41-E
0-250 psi	PX40-250G5V	60	75	DP24-E, DP25-E, DP41-E
0-500 psi	PX40-500G5V	60	75	DP24-E, DP25-E, DP41-E

Ordering Example: PX40-15G5V is a 0-15 psi transducer with .5 to 4.5 Vdc output, \$60



FEATURES



Model 3140

Signal Conditioned Accelerometer
 0.5 to 4.5 VDC Output
 Integral Temperature Compensation
 High Performance

- Vibration/Shock Monitoring
- Geophysical Monitoring
- Modal Analysis
- Structural Analysis
- Elevator Ride Control

DESCRIPTION

The Model 3140 is a high performance accelerometer intended for instrumentation applications. The 3140 provides a fully signal conditioned output with performance similar to traditional instrumentation accelerometers but at a much lower cost.

The accelerometer consists of a silicon micro machined accelerometer with signal conditioning electronics in a lightweight Valox™ housing that can be easily attached to a mounting surface.

The sensing element is a micro machined silicon mass suspended by multiple beams from a silicon frame. Piezoresistors located in the beams change their resistance as the motion of the suspended mass changes the strain in the beams. Silicon caps on the top and bottom of the device are added to provide overrange stops. This design provides for a very low profile, high shock resistance, durability and built-in damping over a wide usable bandwidth.

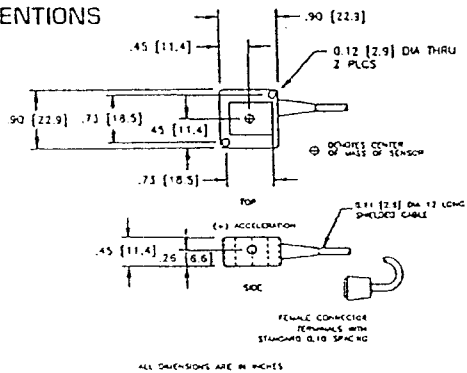
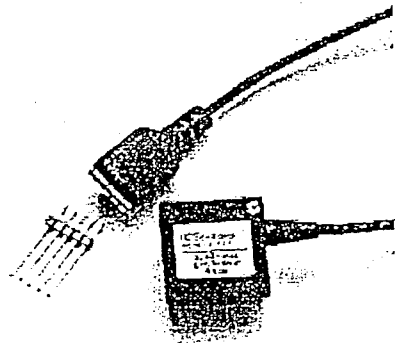
A lower cost version of the 3140 is available for applications that do not require the temperature performance offered with the 3140. Please refer to the Model 3145 for additional information.

FEATURES

- Bolt Mount
- ±0.5% Non-linearity (typical)
- ±2.0% Temperature Performance
- DC Response
- Built-in Damping
- Built-in Overrange Stops
- Low Power

STANDARD RANGES

Range	g
±2	°
±5	°
±10	°
±20	°
±50	°
±100	°



Signal Conditioned Accelerometer

Model 3140

PERFORMANCE SPECIFICATIONS

Supply Voltage: 12 VDC

Ambient Temperature: 25°C (Unless otherwise specified)

PARAMETERS	RANGE					
	±2g	±5g	±10g	±20g	±50g	±100g
Frequency Response [MIN]	0-200	0-300	0-400	0-500	0-600	0-1500
Mounted Resonant Frequency [MIN]	450	600	950	1500	2750	3000
Sensitivity (MIN/MAX)	1 V/g	400mV/g	200mV/g	100mV/g	40mV/g	20mV/g

PARAMETERS	MIN	TYP	MAX	UNITS	NOTES
Full Scale Output Span	3.92	4.00	4.08	Volts	1, 2
Zero Acceleration Output	2.46	2.50	2.54	Volts	1, 2
Accuracy		0.5	1.0	±% Span	3
Transverse Sensitivity		1.0	3.0	±% Span	
Temperature Error - Span (-20 to 85°C)		1.0	2.5	±% Span	2, 4
Temperature Error - Zero (-20 to 85°C)		1.0	2.0	±% Span	2, 4
Supply Voltage	8.0	12.0	30.0	Volts	
Supply Current		5.0		mA	
Reference Voltage		2.5		Volts	5
Output Resistance		0.1		Ω	
Output Noise		0.5		mV p-p	6
Output Load Resistance	5			kΩ	
Acceleration Limits		20X		Rated	
Operating Temperature	-20°C to +85°C				
Storage Temperature	-40°C to +125°C				
Weight (Including Cable)	13 Grams				

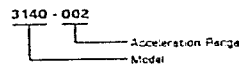
Notes

- The output voltage increases from the Zero Acceleration Output for positive acceleration and decreases for negative acceleration. The sensitivity is then 2V/Range. For example, the ±5g range has a sensitivity of 2V/5g or 400mV/g.
- Actual test data for this parameter is included on the calibration sheet provided with each sensor.
- Includes repeatability, hysteresis, and linearity (best fit straight line).
- Compensated temperature range -20°C to +85°C in reference to 25°C.
- Pin 2 provides an optional 2.5V reference which may be used. If desired, to provide a stable zeroing reference. Thus, the full scale difference output between Pin 2 and Pin 4 would be ±2 VDC. If a single ended output signal is preferred (0.5-4.5

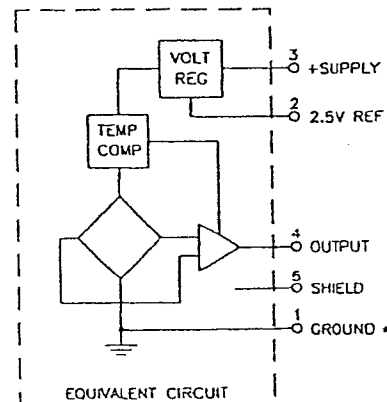
VDC), make no connection to Pin 2. To avoid damage to the internal voltage regulator, do not connect Pin 2 to Pin 1 (gnd). Minimum load resistance connected to Pin 2 without affecting output is 100 kΩ.

- 10 Hz to 1 kHz.
- To use an alternate electrical connection, refer to the following color code for proper electrical connections: Pin 1 - Green; Pin 2 - Yellow; Pin 3 - Red; Pin 4 - Blue; Pin 5 - Shield. Note: Removing the connector voids the product warranty.
- The useful frequency range is defined as the range of frequencies over which the device sensitivity is within ±5% of the DC value.

ORDERING INFORMATION



CONNECTIONS



*Notch on connector to indicate pin one.

Dec 2002
2-29



MICROCHIP

PIC16F87X

28/40-Pin 8-Bit CMOS FLASH Microcontrollers

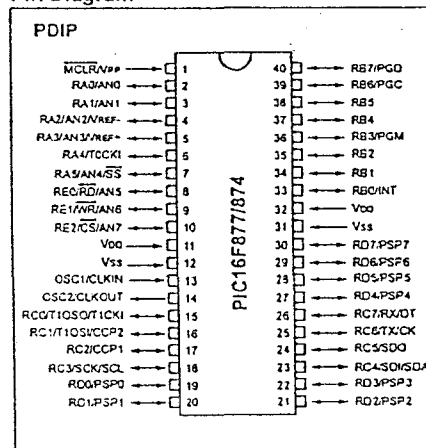
Devices Included in this Data Sheet:

- PIC16F873
- PIC16F876
- PIC16F874
- PIC16F877

Microcontroller Core Features:

- High performance RISC CPU
- Only 35 single word instructions to learn
- All single cycle instructions except for program branches which are two cycle
- Operating speed: DC - 20 MHz clock input
DC - 200 ns instruction cycle
- Up to 8K x 14 words of FLASH Program Memory,
Up to 368 x 8 bytes of Data Memory (RAM)
Up to 256 x 8 bytes of EEPROM Data Memory
- Pinout compatible to the PIC16C73B/74B/76/77
- Interrupt capability (up to 14 sources)
- Eight level deep hardware stack
- Direct, indirect and relative addressing modes
- Power-on Reset (POR)
- Power-up Timer (PWRT) and
Oscillator Start-up Timer (OST)
- Watchdog Timer (WDT) with its own on-chip RC
oscillator for reliable operation
- Programmable code protection
- Power saving SLEEP mode
- Selectable oscillator options
- Low power, high speed CMOS FLASH/EEPROM
technology
- Fully static design
- In-Circuit Serial Programming™ (ICSP) via two
pins
- Single 5V In-Circuit Serial Programming capability
- In-Circuit Debugging via two pins
- Processor read/write access to program memory
- Wide operating voltage range: 2.0V to 5.5V
- High Sink/Source Current: 25 mA
- Commercial, Industrial and Extended temperature
ranges
- Low-power consumption:
 - < 0.6 mA typical @ 3V, 4 MHz
 - 20 µA typical @ 3V, 32 kHz
 - < 1 µA typical standby current

Pin Diagram

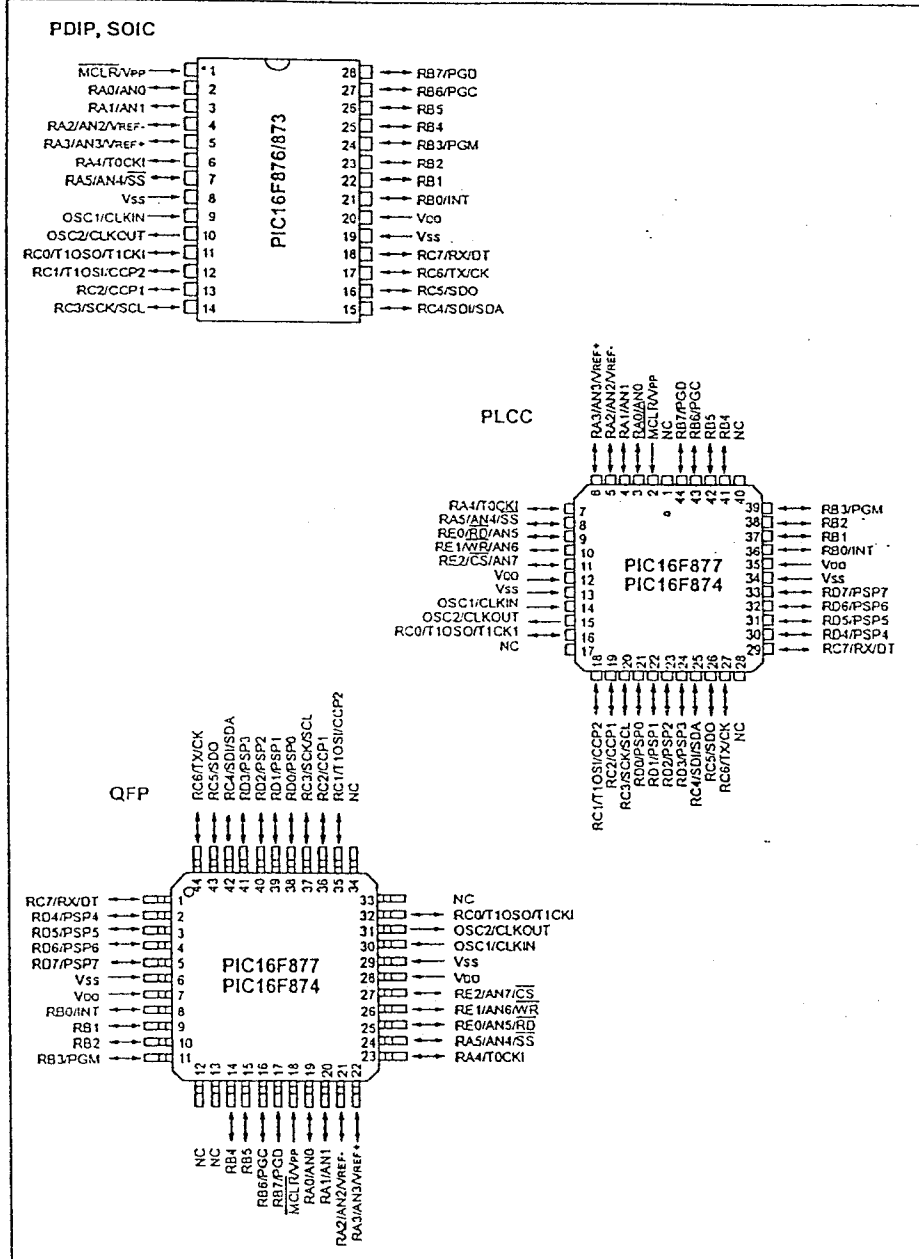


Peripheral Features:

- Timer0: 8-bit timer/counter with 8-bit prescaler
- Timer1: 16-bit timer/counter with prescaler,
can be incremented during SLEEP via external
crystal/clock
- Timer2: 8-bit timer/counter with 8-bit period
register, prescaler and postscaler
- Two Capture, Compare, PWM modules
 - Capture is 16-bit, max. resolution is 12.5 ns
 - Compare is 16-bit, max. resolution is 200 ns
 - PWM max. resolution is 10-bit
- 10-bit multi-channel Analog-to-Digital converter
- Synchronous Serial Port (SSP) with SPI™ (Master
mode) and I²C™ (Master/Slave)
- Universal Synchronous Asynchronous Receiver
Transmitter (USART/SCI) with 9-bit address
detection
- Parallel Slave Port (PSP) 8-bits wide, with
external \overline{RD} , \overline{WR} and \overline{CS} controls (40/44-pin only)
- Brown-out detection circuitry for
Brown-out Reset (BOR)

PIC16F87X

Pin Diagrams



PIC16F87X

Key Features PICmicro™ Mid-Range Reference Manual (DS33023)	PIC16F873	PIC16F874	PIC16F876	PIC16F877
Operating Frequency	DC - 20 MHz			
RESETS (and Delays)	POR, BOR (PWRT, OST)	POR, BOR (PWRT, OST)	POR, BOR (PWRT, OST)	POR, BOR (PWRT, OST)
FLASH Program Memory (14-bit words)	4K	4K	8K	8K
Data Memory (bytes)	192	192	368	368
EEPROM Data Memory	128	128	256	256
Interrupts	13	14	13	14
I/O Ports	Ports A,B,C	Ports A,B,C,D,E	Ports A,B,C	Ports A,B,C,D,E
Timers	3	3	3	3
Capture/Compare/PWM Modules	2	2	2	2
Serial Communications	MSSP, USART	MSSP, USART	MSSP, USART	MSSP, USART
Parallel Communications	—	PSP	—	PSP
10-bit Analog-to-Digital Module	5 input channels	8 input channels	5 input channels	8 input channels
Instruction Set	35 instructions	35 instructions	35 instructions	35 instructions

LMD18200 3A, 55V H-Bridge

General Description

The LMD18200 is a 3A H-Bridge designed for motion control applications. The device is built using a multi-technology process which combines bipolar and CMOS control circuitry with DMOS power devices on the same monolithic structure. Ideal for driving DC and stepper motors; the LMD18200 accommodates peak output currents up to 6A. An innovative circuit which facilitates low-loss sensing of the output current has been implemented.

Features

- Delivers up to 3A continuous output
- Operates at supply voltages up to 55V
- Low $R_{DS(ON)}$ typically 0.3 Ω per switch
- TTL and CMOS compatible inputs

- No "shoot-through" current
- Thermal warning flag output at 145°C
- Thermal shutdown (outputs off) at 170°C
- Internal clamp diodes
- Shorted load protection
- Internal charge pump with external bootstrap capability

Applications

- DC and stepper motor drives
- Position and velocity servomechanisms
- Factory automation robots
- Numerically controlled machinery
- Computer printers and plotters

Functional Diagram

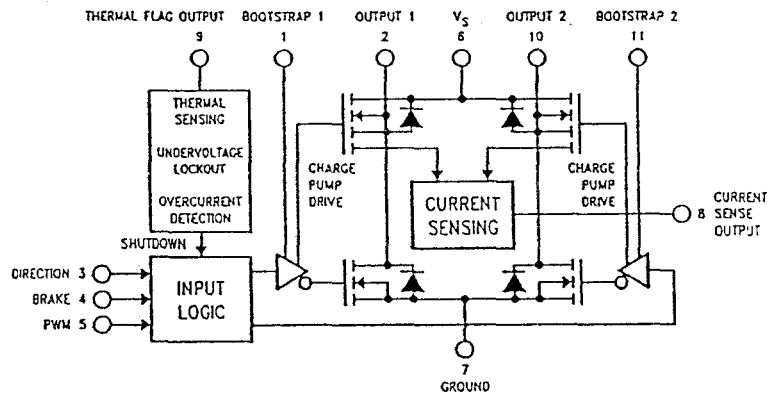
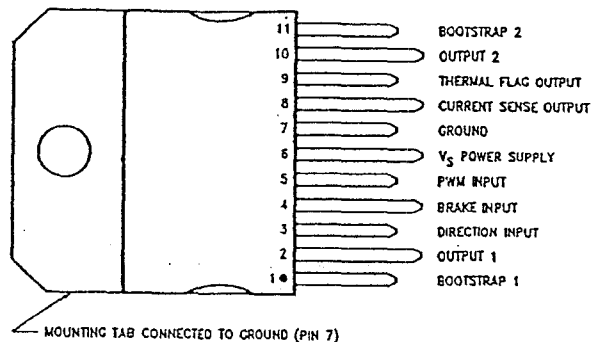


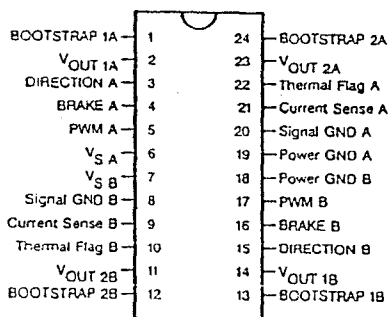
FIGURE 1. Functional Block Diagram of LMD18200

Connection Diagrams and Ordering Information



11-Lead TQ-220 Package
 Top View
 Order Number LMD18200T
 See NS Package TA11B

01056072



24-Lead Dual-in-Line Package
 Top View
 Order Number LMD18200-2D-QV
 5962-9232501VXA
 LMD18200-2D/883
 5962-9232501MXA
 See NS Package DA24B

01010225

LMD18200

Absolute Maximum Ratings (Note 1)

If Military/Aerospace specified devices are required, please contact the National Semiconductor Sales Office/ Distributors for availability and specifications.

Total Supply Voltage (V_S , Pin 6)	60V
Voltage at Pins 3, 4, 5, 8 and 9	12V
Voltage at Bootstrap Pins (Pins 1 and 11)	$V_{CUT} + 16V$
Peak Output Current (200 ms)	6A
Continuous Output Current (Note 2)	3A
Power Dissipation (Note 3)	25W

Power Dissipation ($T_A = 25^\circ C$, Free Air)	3W
Junction Temperature, $T_{J(max)}$	150°C
ESD Susceptibility (Note 4)	1500V
Storage Temperature, T_{STG}	-40°C to +150°C
Lead Temperature (Soldering, 10 sec.)	300°C

Operating Ratings(Note 1)

Junction Temperature, T_J	-40°C to +125°C
V_S Supply Voltage	+12V to +55V

Electrical Characteristics (Note 5)

The following specifications apply for $V_S = 42V$, unless otherwise specified. Boldface limits apply over the entire operating temperature range, $-40^\circ C \leq T_J \leq +125^\circ C$, all other limits are for $T_A = T_J = 25^\circ C$.

Symbol	Parameter	Conditions	Typ	Limit	Units
$R_{DS(ON)}$	Switch ON Resistance	Output Current = 3A (Note 6)	0.33	0.4/0.6	Ω (max)
$R_{DS(ON)}$	Switch ON Resistance	Output Current = 6A (Note 6)	0.33	0.4/0.6	Ω (max)
V_{CLAMP}	Clamp Diode Forward Drop	Clamp Current = 3A (Note 6)	1.2	1.5	V (max)
V_{IL}	Logic Low Input Voltage	Pins 3, 4, 5		-0.1	V (min)
				0.8	V (max)
I_{IL}	Logic Low Input Current	$V_{IN} = -0.1V$, Pins = 3, 4, 5		-10	μA (max)
V_{IH}	Logic High Input Voltage	Pins 3, 4, 5		2	V (min)
				12	V (max)
I_{IH}	Logic High Input Current	$V_{IN} = 12V$, Pins = 3, 4, 5		10	μA (max)
	Current Sense Output	$I_{OUT} = 1A$ (Note 8)	377	325/300	μA (min)
				425/450	μA (max)
	Current Sense Linearity	$1A \leq I_{OUT} \leq 3A$ (Note 7)	± 6	± 9	%
	Undervoltage Lockout	Outputs turn OFF		9	V (min)
				11	V (max)
T_{JW}	Warning Flag Temperature	Pin 9 $\leq 0.8V$, $I_L = 2 mA$	145		$^\circ C$
$V_F(ON)$	Flag Output Saturation Voltage	$T_J = T_{JW}$, $I_L = 2 mA$	0.15		V
$I_F(OFF)$	Flag Output Leakage	$V_F = 12V$	0.2	10	μA (max)
T_{JSD}	Shutdown Temperature	Outputs Turn OFF	170		$^\circ C$
I_S	Quiescent Supply Current	All Logic Inputs Low	13	25	mA (max)
t_{ON}	Output Turn-On Delay Time	Sourcing Outputs, $I_{OUT} = 3A$	300		ns
		Sinking Outputs, $I_{OUT} = 3A$	300		ns
t_{on}	Output Turn-On Switching Time	Bootstrap Capacitor = 10 nF			
		Sourcing Outputs, $I_{OUT} = 3A$	100		ns
		Sinking Outputs, $I_{OUT} = 3A$	80		ns
t_{OFF}	Output Turn-Off Delay Times	Sourcing Outputs, $I_{OUT} = 3A$	200		ns
		Sinking Outputs, $I_{OUT} = 3A$	200		ns
t_{off}	Output Turn-Off Switching Times	Bootstrap Capacitor = 10 nF			
		Sourcing Outputs, $I_{OUT} = 3A$	75		ns
		Sinking Outputs, $I_{OUT} = 3A$	70		ns
t_{DWR}	Minimum Input Pulse Width	Pins 3, 4 and 5	1		μs
t_{CDR}	Charge Pump Rise Time	No Bootstrap Capacitor	20		μs



